



Trans. Nonferrous Met. Soc. China 28(2018) 1980-2001

Transactions of **Nonferrous Metal** Society of China

www.tnmsc.cn



Recent advances in pseudocapacitor electrode materials: Transition metal oxides and nitrides

Chen-qi YI, Jian-peng ZOU, Hong-zhi YANG, Xian LENG State Key Laboratory of Powder Metallurgy, Central South University, Changsha 410083, China Received 29 June 2017; accepted 14 December 2017

Abstract: Faraday pseudocapacitors take both advantages of secondary battery with high energy density and supercapacitors with high power density, and electrode material is the key to determine the performance of Faraday pseudocapacitors. Transition metal oxides and nitrides, as the two main kinds of pseudocapacitor electrode materials, can enhance energy density while maintaining high power capability. Recent advances in designing nanostructured architectures and preparing composites with high specific surface areas based on transition metal oxides and nitrides, including ruthenium oxides, nickel oxides, manganese oxides, vanadium oxides, cobalt oxides, iridium oxides, titanium nitrides, vanadium nitrides, molybdenum nitrides and niobium nitrides, are addressed, which would provide important significances for deep researches on pseudocapacitor electrode materials.

Key words: pseudocapacitor; transition metal oxides; transition metal nitrides; energy density; power density

1 Introduction

With the expansion of the information society and the appearance of the energy crisis, energy storage and conversion are becoming more and more important. Among the various energy conversion systems, electrochemical power sources have been widely used since they exhibit the highest energy conversion efficiency. Batteries [1] and supercapacitors are two kinds of typical electrochemical power sources. Supercapacitors are also known as electrochemical capacitors, which include electric double-layer capacitors (EDLCs) and Faraday pseudocapacitors. In the 1980s, NEC Corporation started to prepare supercapacitor products, heralding the era of commercial supercapacitor applications. Supercapacitors exhibit high power density, long cycle life, quick charging rate, relatively high safety, eco-friendliness and more suitable for charging and discharging under high power conditions than batteries [2], and can be applied as back-up power, start-up power, electrical network balance power, pulse power and so on [3]. The power characteristics of supercapacitors change little during long-term storage compared with those of batteries, hence supercapacitors can also work as hybrid power supply systems combined with nickel-metal hydride batteries, lithium-ion batteries or fuel cells to improve efficiency and lifetime.

The major shortcoming of supercapacitors is that their energy density is much lower than that of secondary batteries represented by lithium-ion batteries. Therefore, improving the energy density is one of the major objectives of the supercapacitor research field.

Improving the energy density of a supercapacitor generally starts from the following two approaches. First is to promote the manufacturing technique of supercapacitors by reducing the amount of attachment, including electrolyte membrane, current collector and the capacitor cases, and increasing the amount of electrode materials. Second is to improve the energy density of the electrode materials. The latter is the key issue since the manufacturing technology of supercapacitors is basically fixed and attachment reduction is difficult to achieve.

According to the supercapacitor energy calculation formula, $E=1/2CU^2$, improving the working voltage (U) and capacitance (C) is an effective way to improve the supercapacitor energy density. However, due to the limits of breakdown voltage of the electrolyte, the working voltage of a single supercapacitor is very low. More specifically, the working voltages of a single supercapacitor in an aqueous or organic electrolyte are no more than 2 and 3 V, respectively. Undoubtedly, the working voltage can be improved by placing the capacitor units in series. Using an electric vehicle as an example, high working voltage requirements need hundreds of units in series. Thereby, the overall capacitance will decrease and the equivalent series resistance will increase by series. However, such a large series can easily breakdown locally due to the differences in the performances and parameters among different units, finally breaking down drastically overall. Thus, increasing the energy density of supercapacitors mainly depends on improving the specific capacitance.

EDLCs, whose energy storage has been achieved by double-layer capacitance at the interface between electrodes and electrolytes [4], mainly use carbon-based materials with high specific surfaces. In general, the specific capacitance of EDLCs is not high since their density is low.

Compared with EDLCs, Faraday pseudocapacitors exhibit much larger specific capacitance since the capacitance takes place both at the interfaces and in the bulk of the electrode materials. Thus, pseudocapacitors can improve the energy density greatly. The energy storage mechanism is based on the highly reversible redox reaction in the electrodes [5]. Differing from the completely reversible process of physical chargecharge-desorption absorption pseudocapacitors are irreversible partially due to the involvement of chemical reaction processes in the electrodes, which leads to their relatively poor cycling performance and rate capability. Nowadays, the mainstream direction of capacitor research is to improve the energy and power densities simultaneously, so pseudocapacitor is an excellent choice. Supercapacitors have attracted considerable attention from researchers and the number of publications on pseudocapacitors has increased rapidly in recent years (Fig. 1).

Pseudocapacitor electrode materials mainly belong to three categories: transition metal oxides, transition metal nitrides and conductive polymers. Conductive polymers include polyaniline (PANI), polythiophene (PT) and polypyrrole (PPY), which possess long-chain conjugated double bonds. The obvious shortcoming of conductive polymers is that their conductivity is relatively low, which makes their rate performance and capacitance capability poorer. The practical capacitances of PANI, PT and PPY are only 150-190 F/g [6,7], 78-117 F/g [8,9] and 80-100 F/g [10,11], respectively, which are much lower than the expected values and can hardly meet practical needs. Transition metal oxides and nitrides show great potential in capacity performance. Thus, a timely and comprehensive review of transition metal oxides and nitrides is addressed in this work.

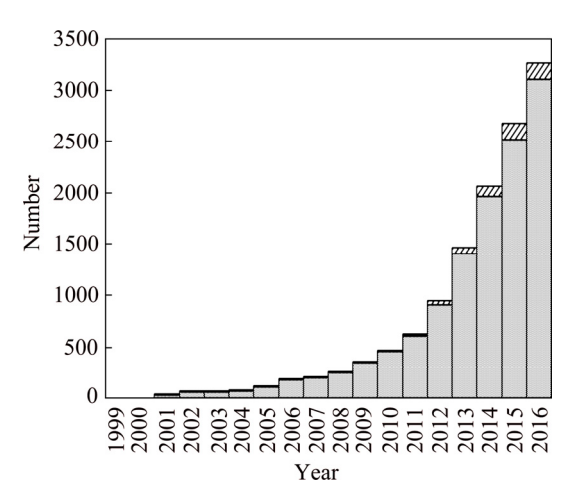


Fig. 1 Trends in number of publications on supercapacitors () and pseudocapacitors () (data obtained from Web of Science on January 19th, 2017)

A significant amount of researches have been completed on pseudocapacitor material target strategies to improve the electrochemical performance of these devices, which is often achieved through the formation of composite materials [12]. Composites of carbon with redox active materials, prepared by the insertion of electroactive particles of transition metal oxides or nitrides into the carbon materials [13], have been evaluated as electrode materials for electric capacitors and show improved performance. Various approaches have been proposed to synthesize well-defined electrode networks to minimize the resistivity, as shown as in Fig. 2. The same strategy can be applied for most pseudocapacitor electrode materials.

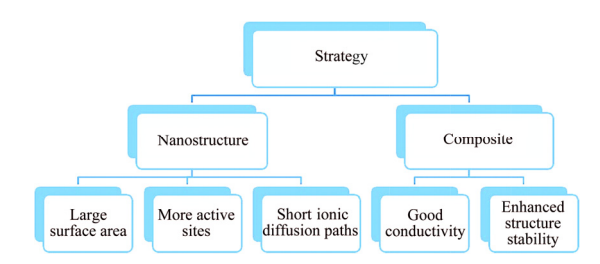


Fig. 2 Strategy for enhancing performance of pseudocapacitors [14]

2 Transition metal oxides

Transition metal oxides, including RuO₂, MnO₂, NiO, V₂O₅, Co₃O₄ and IrO₂, undergo fast reversible redox reactions on their surface (Fig. 3) and displaying strong pseudocapacitive behavior. The reversibility of these electrodes can be indicated by cyclic voltammetry (CV) curves, which shows that the symmetric redox peaks are dramatically different from the rectangular CV curves seen in EDLCs (Fig. 4). These oxides have been extensively studied as their capacitance usually greatly

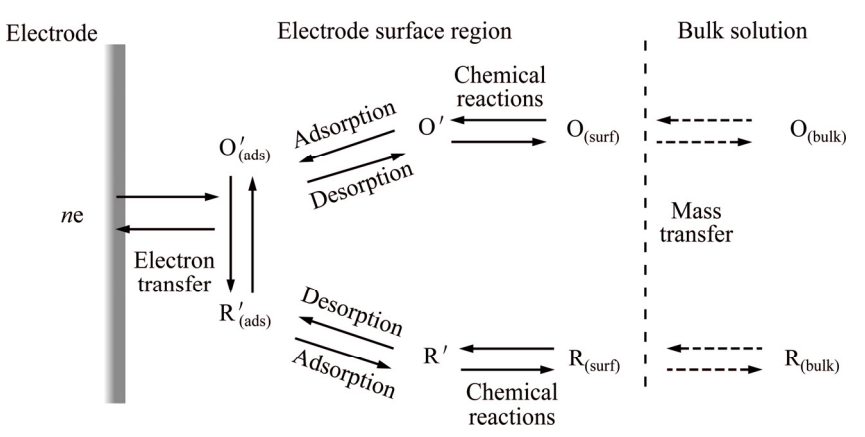


Fig. 3 Schematic diagram of reversible redox reaction at electrode/electrolyte interface leading to pseudocapacitance [15]

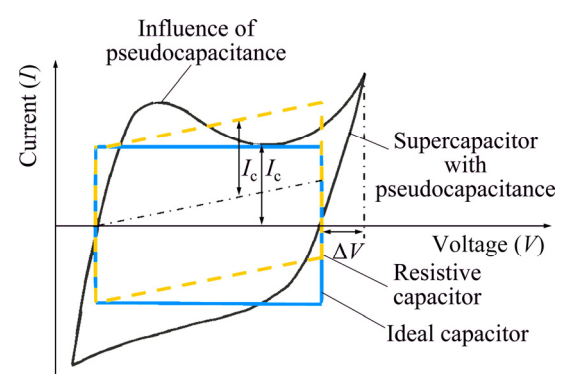


Fig. 4 Fundamental difference between current curves of EDLCs and pseudocapacitors [16]

exceeds the double-layer capacitance achievable with carbon materials. The theoretical capacitances of RuO_2 , MnO_2 , NiO, V_2O_5 and Co_3O_4 are 2200, 1370, 2584, 2120 and 3560 F/g (Fig. 5), respectively, which makes the energy density of transition metal oxides very attractive.

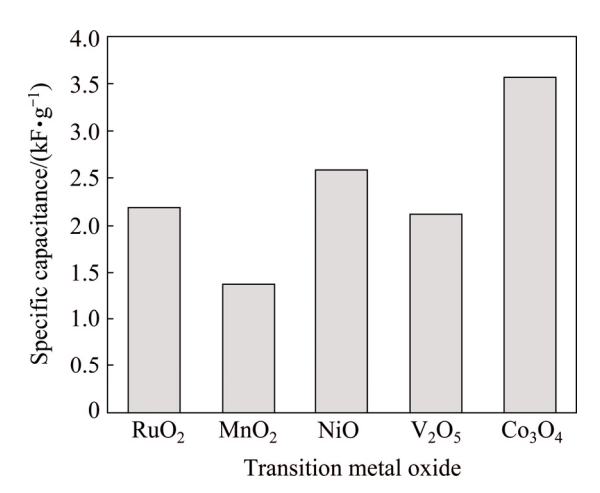


Fig. 5 Theoretical capacitances of different transition metal oxides

2.1 Ruthenium oxides

Nanocrystalline hydrous ruthenium dioxide (RuO₂·xH₂O), as an excellent pseudocapacitor electrode

material, is widely known for its extremely high theoretical specific capacitance, good electronic conductivity, excellent thermostability and chemical stability. RuO₂ prepared by thermal decomposition (350-550 °C) of RuCl₃·3H₂O showed an enhanced total cathodic and anodic charging ability and featureless voltammetric curves, quite different from the redox process of RuO2 single crystals, which was first discovered by TRASATTI and BUZZANCA [17]. The electrically conductive RuO₂·xH₂O [18] prepared via a sol-gel method exhibited a reasonably large specific capacitance of 720 F/g through a proton migration process, at least twice as high as crystalline RuO2, and opened a new insight in fabricating high-energy density electrochemical capacitors. Tremendous efforts have been continuously geared to understand the influence of precursors of the heating process, which determine the crystallinity, exposed crystal phase, structural water content, particle size and specific surface area of as-prepared products, on the electrochemical capacitance and underlying mechanism.

Various methods, such as chemical deposition, pulsed laser deposition, electrostatic spray deposition, anodic deposition and hydrothermal processing [19-21], have been developed to prepare RuO₂ films or powders featuring a highly reversible redox reaction, a wide potential window (1.2 V) and good thermal and chemical stability. For example, DESHMUKH et al [22] deposited RuO₂·nH₂O thin film through a simple chemical bath process, and it revealed 41.6 W·h/kg and 1.5 kW/kg at 300 μA/cm² with 95% Coulombic efficiency. ADAMS et al [23] summarized the conductivity and capacitive properties of RuO₂, derived from the single crystal to a highly disordered structure (Fig. 6).

$$RuO_2 + xH^+ + xe \rightleftharpoons RuO_{2-x}(OH)_x (0 \le x \le 2)$$
 (1)

As for the preparation of RuO₂, the increase of accessible surface, the formation of highly ordered or

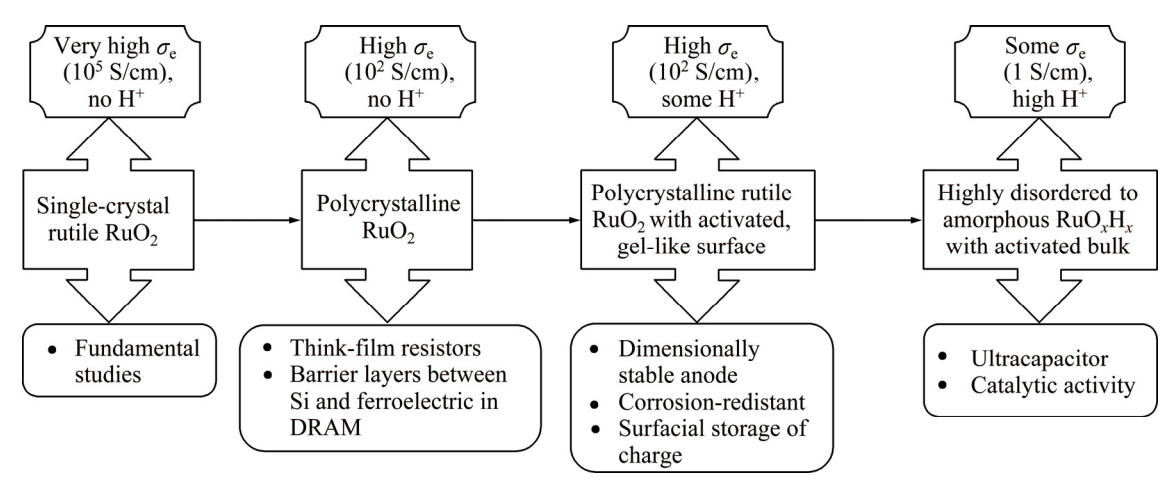


Fig. 6 Ruthenium dioxides—An example of spectrum of properties with different crystal structures [23]

hollow structures and the exploration of optimum annealing conditions are major factors for achieving high practical specific capacitance [24] and superior rate capability. Therefore, versatile hard templates (a mesoporous silica template [25], α -Fe₂O₃ [26] and MnOOH [27]) and/or surfactants acting as soft templates or pore-directing agents [28], were adopted to construct three-dimensional (3D) nanoporous or mesoporous networks for fast electron and ion transportation. WU et al [26] prepared hollow RuO₂·xH₂O with α-Fe₂O₃ sacrificial template and it exhibited 772, 671, 502 and 360 F/g at 0.5, 4, 20 and 40 A/g, respectively, which also experienced an activation period and achieved 823 F/g after 1000 cycles at 1 A/g. ZHANG et al [27] proposed the mechanism of forming nanotubular RuO₂ from a sacrificial template of manganite nanorods, which showed 861, 787, 722 and 654 F/g at 0.5, 1, 2 and 4 A/g, respectively, benefiting from the reduced resistance of electrolyte penetration and diffusion. JEONG et al [29] electrochemically deposited hydrous ruthenium oxide with open pores and numerous dendritic morphologies with a dynamic hydrogen template, with capacitance of 809 F/g at 1.5 A/g. LIN et al [28] fabricated a 3D mesoporous crystalline RuO2 film with enhanced electrochemical active centers via an evaporationinduced self-assembled method, which exhibited an ultrahigh power density with an acceptable energy density.

Layered ruthenic acid, $H_{0.2}Ru_{2.1}\cdot nH_2O$ (HRO), featuring a crystalline ruthenium oxide layer interleaved with water, shows comparable inner electronic conductivity with rutile RuO_2 and similar capacitive performance to hydrous RuO_2 , benefiting from the utilization of the interlayer surface and surface active sites [30]. SUGIMOTO et al [31] revealed that pristine HRO reached 392 and 329 F/g at 2 and 500 mV/s, respectively, while exfoliated HRO exhibited 658 and 601 F/g at 2 and 500 mV/s, respectively. Other

elaborately designed electrode constructions have also been developed. HYUN et al [32] electrochemically deposited RuO2·nH2O overlayers on conductive crystalline RuO₂ (~10 nm) fibers, which showed 886.9 F/g at 10 mV/s based on the mass of RuO₂·nH₂O, corresponding to 104.3 F/g based on the total mass of RuO₂ fiber mats and RuO₂·nH₂O coating layer. SUSANTI et al [33] encased anhydrous RuO2 nanorods with hydrous RuO₂ via an electrochemical deposition. The annealed structure revealed 526 F/g (878 mF/cm²) at 5 mV/s, which decreased to 78.6 F/g (131 mF/cm²) at 500 mV/s. When metallic Pt was used as the core, significantly improved capacity retention at high discharge rates seemed to be achieved. PONROUCH et al [34] fabricated Pt@RuO₂ core-shell nanotube arrays for micro-supercapacitor electrodes, which demonstrated 320 and 256 mF/cm² at 2 and 500 mV/s, respectively, with ~80% capacity retention. RYU et al [35] constructed transparent supercapacitors by electrodepositing hydrous RuO₂ on 1D indium tin oxide (ITO) nanopillars, and a maximum specific capacitance of 1235 F/g at 50 mV/s was achieved, which also showed excellent capacitance retention of ~94.3% from 10 to 200 mV/s. A schematic representation of the construction of the coaxial ITO core-RuO2 shell nanopillar electrode is shown in Fig. 7.

The commercial of RuO₂-based electrodes used in supercapacitors is seriously hindered by the high cost of RuO₂. Therefore, a number of studies have focused on composing RuO₂ with other materials that store charge through double layers and reversible redox processes. Combining RuO₂ with carbon materials has several advantages [36]: 1) Carbon materials can work as a matrix possessing a high surface area to disperse and lower the size of RuO₂ particles, which creates higher utilization; 2) A porous carbon support can accelerate the transporting rate of ions into the bulk of the electrode, or act as an "electrolyte reservoir" that prevents depletion

or oversaturation of protons at high voltage scans, which would improve the power performance; 3) Wellcrystallized carbon might also reduce the contact resistance between RuO₂ particles and enhance the conductivity of RuO₂/carbon composites. Various forms of carbon materials have been investigated to achieve these benefits, such as carbon aerogel, activated carbon, carbon black, carbon nanofibers, carbon nanotubes and carbon spheres [37-39]. AN et al [40] prepared surface-modified RuO₂/carbon nanofiber composites, which exhibited outstanding energy densities of 26.9-21.5 W·h/kg at 349.0-17545.5 W/kg, and a cycle stability of 90% after 3000 cycles, owing to the well-connected structure and the synergistic effect from the two components. HSIEH et al [41] electrochemically deposited (50 mV/s) hydrous RuO2 on multi-walled carbon nanotubes, and the composite revealed excellent specific capacitances of 1652 and 863 F/g at 10 and 500 mV/s, respectively. WANG et al [42] adopted a core-shell template approach to fabricate carbon or carbon nanotube-supported hollow RuO2 nanoparticles (referred to as hRuO₂/C and hRuO₂/CNT, respectively) for supercapacitor electrodes. The hRuO2/C and hRuO₂/CNT reached 817.1 and 819.9 F/g at 0.2 A/g, and retained 750.4 and 655.0 F/g at 5 A/g, respectively. The power and energy densities achieved by the hRuO2/C and hRuO₂/CNT were 427.6 W/kg and 133.8 W·h/kg, and 557.3 W/kg and 127.9 W·h/kg, respectively, which showed the advantages of the hollow nanostructure. A schematic illustration of hRuO2/C and hRuO2/CNT and the corresponding TEM images are presented in Fig. 8. The core-shell hybrid of the RuO2-coated carbon nanotubes composite [38] also exhibited a competing performance of 11.9 W·h/kg at 3000 W/kg. When switching the role of RuO₂ and the carbon support, a RuO₂ matrix decorated with carbon quantum dots reported by ZHU et al [43] reached 594 F/g at 1 A/g, and ultrahigh rate capabilities of 88.6%, 84.2%, and 77.4% capacity retention at 10, 20 and 50 A/g, respectively.

Introducing RuO2 to graphene, which features a 2D nanostructure, could prevent the agglomeration of RuO₂ or the stacking of graphene sheets, thus providing more electrolyte accessible surface. Some RuO2-graphene composites have been prepared through sol-gel or hydrothermal methods. WU et al [44] pioneered the synthesis of RuO₂/graphene, the sample with 38.3% Ru loading showed 570 F/g at 1 mV/s, and a high energy density of 20.1 W·h/kg at 50 W/kg and a superior power density of 10 kW/kg at 4.3 W·h/kg. DINH et al [45] fabricated on-chip micro-supercapacitors based on RuO₂/ carbon nanowalls (consisting of graphene domains), which delivered 1094 mF/cm² at 2 mV/s and a high energy density of 49 (µW·h)/cm². The electrochemical performance of these micro-supercapacitors comparable to state-of-the-art lithium-ion micro-batteries. A new trend is to combine transition metal oxides with different types of carbon materials to form a ternary composite to enhance the energy and power densities simultaneously. The backbone of graphene/CNT for depositing RuO₂ can be formed through chemical vapor deposition (CVD) or wet chemistry. WANG et al [46] deposited a graphene/MWCNT foam via CVD and subsequently dip-coated it with RuO₂ suspension to form a RuO₂/graphene/CNT hybrid (RGM). The schematic

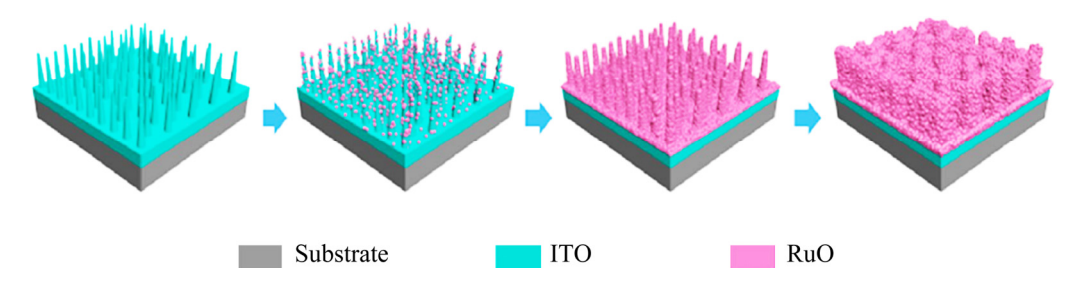


Fig. 7 Schematic diagram of construction of coaxial ITO core-RuO₂ shell nanopillar electrode [35]

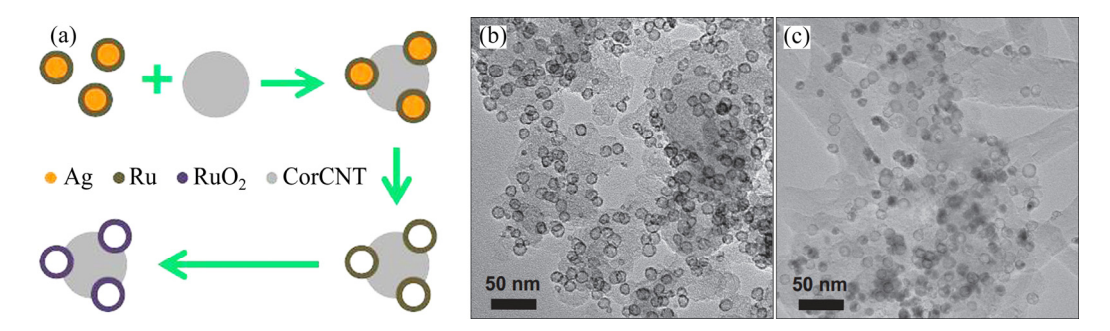


Fig. 8 Schematic illustration of C- or CNT-supported RuO₂(a) and TEM images of hRuO₂/C (b) and hRuO₂/CNT (c) [42]

illustration of the preparation process is shown in Fig. 9. The RGM showed the highest gravimetric and per-area capacitive performance of 502.8 F/g and 1.1 F/cm², and it exhibited an exceptionally high energy density of 39.3 W·h/kg and a power density of 128.0 kW/kg. HU et al [47] also explored the applicability of graphene/ CNT/RuO₂ composites for fabricating supercapacitor electrodes. The composite annealed at 150 °C exhibited 135 W·h/kg and 12 kW/kg, and the corresponding symmetric supercapacitor delivered 33.8 W·h/kg and 3 kW/kg.



Fig. 9 Schematic illustration of fabrication of RGM nanostructure foam [46]

In order to enhance the utilization of RuO₂ in pseudocapacitance storage at a more reasonable cost, inorganic oxides with promising pseudocapacitance or metallic conductivity, such as MnO₂, NiO, Co₃O₄, SnO₂, TiO₂, Ta₂O₅, SrRuO₃ and ZrO₂, have been incorporated with RuO₂ to form hybrid electrodes. CHOU et al [48] chemically deposited a MnO₂ coating on 1D RuO₂ nanorods through a radio-frequency magnetron sputtering system. The RuO₂/MnO₂ core-shell nanorods with a good rate capability reached 793 F/g at 2 mV/s and 556 F/g at 1 A/g. RAKHI et al [49] electrodeposited nanocrystalline, hydrous RuO₂ to mesoporous Co₃O₄ to form a RuO₂/Co₃O₄ composite with enhanced rate

performance. The RuO₂/Co₃O₄ with the optimal RuO₂ electrodeposition time resulted in 905 F/g at 1 A/g and a high retention of 78% at 40 A/g. BRUMBACH et al [50] fabricated ruthenium oxide-niobium hydroxide composites with varying precursor ratio. As the niobium hydroxide worked as an effective proton conductor and induced a decrease in RuO₂ particle size, the energy storage of Nb:Ru composites with only half to a third of Ru exceeded that of the pure RuO₂ electrode.

Many conductive polymers with high pseudocapacitance, have also been incorporated with RuO2 to alleviate the aggregation of RuO₂ and improve its mechanical stability. DESHMUKH et al [51] prepared a PANI-RuO₂ composite thin film via a chemical bath deposition. The growth mechanism is shown in Fig. 10. The PANI-RuO₂ composite thin film exhibited 830 F/g at 5 mV/s, and a specific energy and power of 216 W h/kg and 4.2 kW/kg, respectively. The same group [52] also synthesized a polyaniline-ruthenium oxide composite via a successive ionic layer adsorption and reaction method, and it yielded 664 F/g at 5 mV/s. CHO et al [53] designed a ternary flexible system based on a RuO₂ nanoparticle-decorated PEDOT:PSS/graphene nanocomposite, which exhibited 820 F/g at 0.5 A/g and 73 W·h/kg at 67 W/kg.

2.2 Nickel oxides

Nickel oxide (NiO) has been suggested to be the optimal alternative material for pseudocapacitors because of its lower cost and more environmental friendliness when compared to RuO₂ [16]. It has an unusually high theoretical specific capacitance [54] and higher electrical conductivity compared to other metal oxides/hydroxides or polymers [55], as well as a high surface area, making it very attractive as an electrode material for

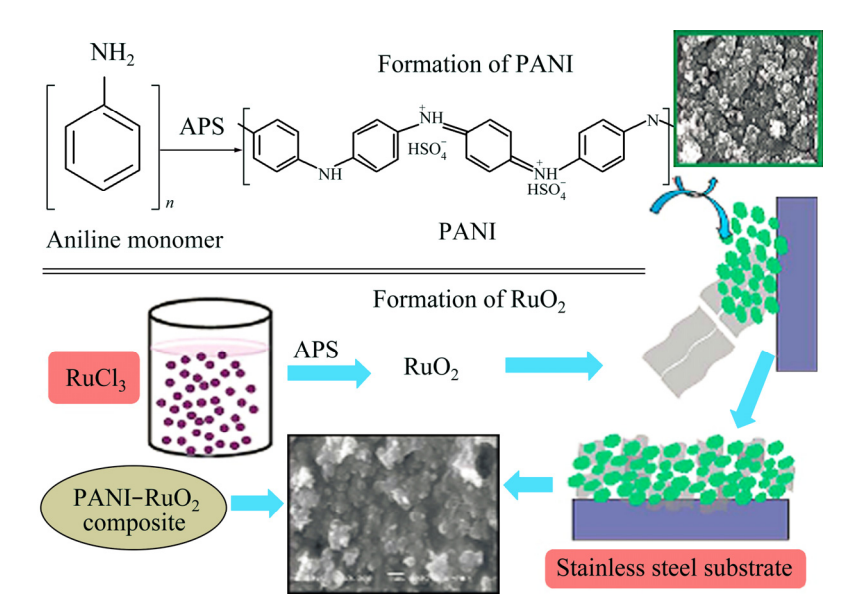


Fig. 10 Growth mechanism of PANI–RuO₂ composite thin film [51]

pseudocapacitors. As a result, many effective efforts have been devoted to synthesizing different morphologies of NiO nanomaterials by various wet chemical methods, such as nanoparticles, nanoplates, hollow octahedrons and complicated hierarchical nanostructures [56,57].

The capacitance of NiO mainly results from a fast redox reaction according to the following equation:

$$NiO+OH \Longrightarrow NiOOH+e$$
 (2)

However, the real specific capacitance obtained from NiO materials is far below its theoretical value because of its high resistance (less than 10⁻¹ S/cm at room temperature [58]). ZHANG et al [59] synthesized porous NiO nanostructures with a specific capacitance of 390 F/g at a discharge current of 5 A/g. VIJAYA-KUMAR et al [60] adopted a microwave route to prepare NiO nanoflakes, which exhibit a specific capacitance of 401 F/g at a current density of 0.5 mA/cm². Therefore, it is desirable to produce electrode materials with high specific surface areas as well as suitable pore size distributions (2–5 nm) to improve the specific capacitance of pseudocapacitors.

By decorating NiO nanostructures on graphene foam [61], the composite exhibited an increased electrochemical performance of about 1225 F/g at 2 A/g. LU et al [62] reported a simple, cost-effective and potentially scalable technique for fabricating monolithic NiO/Ni nanocomposite electrodes with a remarkably high specific capacitance of 900 F/g. Moreover, WANG et al [16], reported a novel approach to synthesize hierarchical composite electrodes of nickel oxide nanoflakes with 3D graphene for high-performance pseudocapacitors, with a remarkable specific capacitance of 1829 F/g at a current density of 3 A/g. In their study, NiO nanoflakes were created with a simple hydrothermal method on 3D graphene scaffolds grown on Ni foams by microwave plasma enhanced chemical vapor deposition. Such as-grown NiO-3D graphene composites (NGC) were then applied as monolithic electrodes for a pseudocapacitor application without the requirement for binders or metal-based current collectors. Another nickel-based material, Ni(OH)2, is also the most promising candidate for supercapacitors with its high theoretical specific capacitance of 2082 F/g [63].

Encouraged by its remarkable potential application, effective efforts have been devoted to the synthesis of Ni(OH)₂ nanostructures with different morphologies and structures, such as platelet-like, flower-like, nanoparticles, microspheres, nanotubes and nanorods [64–66]. Among these different morphologies, flower-like nanostructured Ni(OH)₂ has attracted considerable attention because of its short diffusion path lengths for both electrolyte ions and electrons, favoring

the diffusion and migration of electrolyte ions during the rapid charge/discharge process, consequently improving its effective electrochemical utilization [67]. Furthermore, the composite coupled with graphene exhibits high specific capacitance. WANG et al [63] synthesized Ni(OH)₂ nanocrystals grown on graphene sheets (NGS) with various degrees of oxidation (Fig. 11), which exhibited a high specific capacitance of 1335 F/g at a charge and discharge current density of 2.8 A/g.

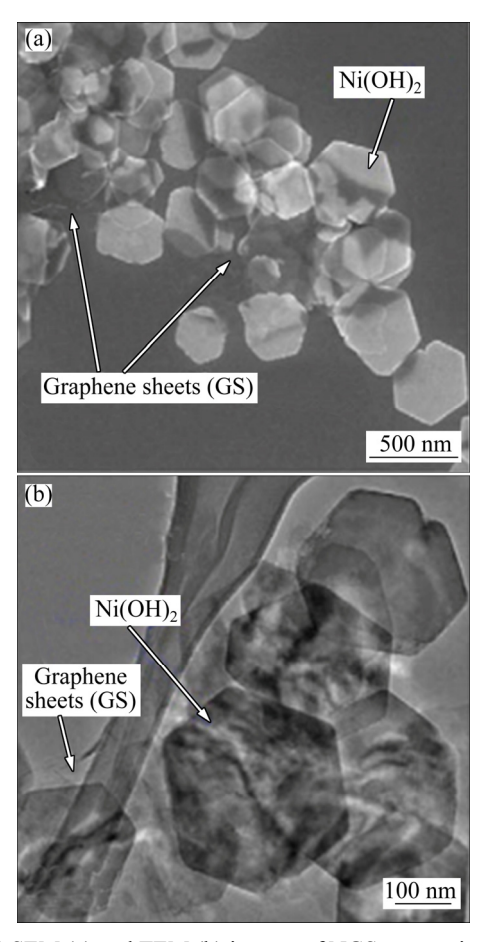


Fig. 11 SEM (a) and TEM (b) images of NGS composite [63]

YAN et al [68] reported a novel strategy to prepare hierarchical flower-like Ni(OH)₂ decorated on graphene sheets using a fast, facile and cost-effective microwave heating method without any templates or additional agents. The Ni(OH)₂/graphene hybrid exhibited a high specific capacitance of 1735 F/g and high rate capability compared to a pure Ni(OH)₂ electrode (Fig. 12).

A comparison of some experimental results for the NiO redox couple is shown in Table 1. With different morphologies of NiO or Ni(OH)₂ materials, a broad range of capacitance from 124 to 1335 F/g can be obtained. The crystal phase, structural morphology and surface area are of critical importance for the development of high performance electrochemical energy storage devices with simultaneous high energy and power densities.

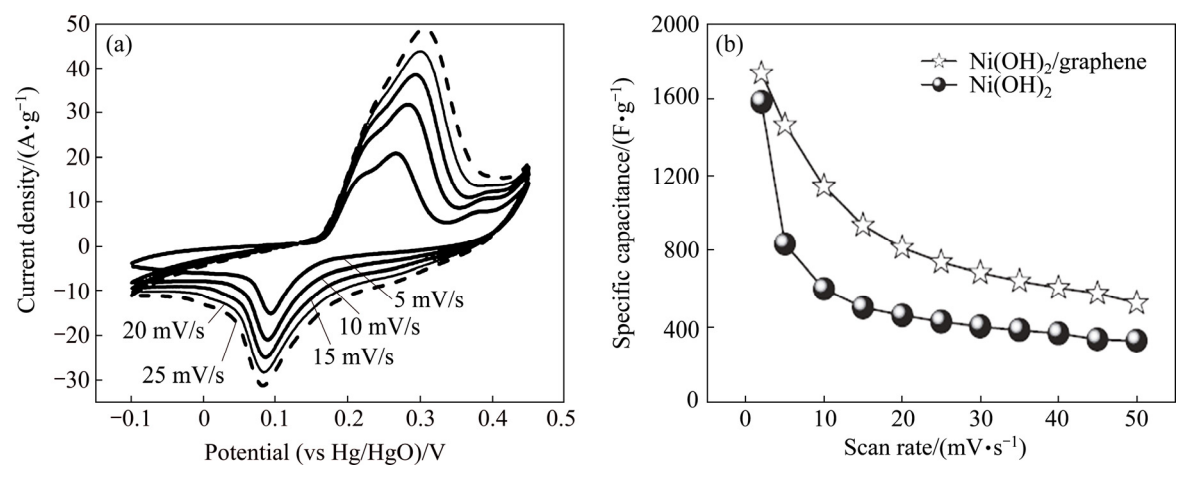


Fig. 12 CV curves of Ni(OH)₂/grapheme composite at various scan rates in 6 mol/L KOH (a) and specific capacitance of pure Ni(OH)₂ and Ni(OH)₂/graphene composite as function of scan rate based on CV curves (b) [68]

Table 1 Comparison of experimental results for NiO redox couple [69]

to the second sec								
Material	Phase	Morpholopy	$Capacitance/(F \cdot g^{-1})$	Surface area/ $(m^2 \cdot g^{-1})$	Electrolyte			
NiO	Cubic	Porous ball	124	477	3% KOH			
NiO	Cubic	Nanoflake	140	108	2 mol/L KOH			
NiO	Cubic	Thin film	590		3% KOH			
NiO	Cubic	Thin film	1110		1 mol/L KOH			
NiO	Monoclinc	Petal	710	216	6 mol/L KOH			
		Nanocolumn	390	103				
NiO	Monocline	Nanoslice	285	20	1 mol/L KOH			
		Nanoplate	176	11				
NiO	Cubic	Nanoflake	411	227	2 mol/L KOH			
NiO-MWNT	Cubic	Nanoflake	206	228	2 mol/L KOH			
Ni(OH) ₂ on activated carbon	β -Ni(OH) ₂	Irregular	194	134	6 mol/L KOH			
Ni(OH) ₂ on activated carbon	β -Ni(OH) ₂	Nanopaticle	315		6 mol/L KOH			
Ni(OH) ₂ on graphene	β -Ni(OH) ₂	Nanopaticle	1335		1 mol/L KOH			

2.3 Manganese oxides

Manganese dioxide (MnO₂) has a high theoretical specific capacitance of 1370 F/g [70] and is considered to be one of the alternatives for pseudocapacitors. The pseudocapacitive behavior of MnO₂ was first studied by LEE and GOODENOUGH in 1999 [71]. Porous hydrous MnO₂, which has been facilely and widely prepared by the organic-aqueous interfacial method [72], exhibits a capacitance of 261 F/g and good cyclic performance, but only at low charge/discharge rates, showing that pure manganese oxide cannot be applied for capacitor applications.

Recently, many research efforts have been focused on its compounds in order to provide high charge/discharge rates. The mechanism of MnO₂ charge storage behavior can be explained according to Eq. (3) [73].

$$MnO_2+H^++e \longrightarrow MnOOH$$
 (3)

However, the performance of MnO_2 supercapacitors is very disappointing, only less than 30% of the theoretical capacitance of MnO_2 (<100–300 F/g) can be retained [74] since its electrochemical properties strongly depend on its dimensionality, powder morphology, crystalline structure and bulk density [75]. In addition, the poor conductivity of MnO_2 (1×10⁻⁵–1×10⁻⁶ S/cm) also limits the charge/discharge rate for high-power applications [76].

Thus, many studies have been carried out to synthesize reasonable structures and compositions of MnO₂ for the purpose of improving electrolyte access and electron transportation. LANG et al [77] synthesized hybrid structures (NPG/MnO₂) made of nanoporous gold (NPG) and nanocrystalline MnO₂, exhibiting a specific capacitance of 1145 F/g, acting as a double-layer

capacitor. This high specific capacitance is attributed to the nanoporous gold, which not only allows electron transport through the MnO₂, but also facilitates fast ion diffusion between MnO₂ and the electrolytes.

By using hydrothermally synthesized α -MnO₂ nanowires, OZKAN et al [78] uniformly coated on graphene/multi-walled carbon nanotube (GM) foam. The GM foam was grown on nickel foam (NF) via ambient pressure chemical vapor deposition. Symmetrical ECs based on graphene/multi-walled carbon nanotube/MnO₂ nanowire (GMM) foam electrodes show an extended operational voltage window of 1.6 V in aqueous electrolyte, which also exhibit an excellent specific capacitance of 1109 F/g.

2.4 Vanadium oxides

Vanadium pentoxide (V_2O_5) is a favorable candidate as a supercapacitor electrode because of its accessible layered structure, high potential (about 3 V), high specific capacity, mixed valence states (V^{2+} , V^{3+} , V^{4+} and V^{5+}), low cost, easy procedure for synthesis and nontoxic chemical properties [79].

There are many methods used to obtain different nanostructures of V_2O_5 or VO_2 , such as hydrothermal, electrospinning, sol-gel and template-assisted growth [80–82]. The various synthesized nanostructures of V_2O_5 or VO_2 also have been applied in a variety of fields, including sensors, optical switching devices, optical data storage media and electrode materials for Li-ion batteries [83]. The V_2O_5 bulk lattice are shown in Fig. 13. Equation (4) implies the intercalation of protons (H⁺) in the bulk of the material upon reduction:

$$V_2O_5 + xH^+ + xe \rightleftharpoons V_2O_{5-x}(OH)_x \tag{4}$$

The electrochemical properties of vanadium oxide were evaluated by CV measurements at various scan rates in electrolytes. WEI et al [85] synthesized vanadium oxide nanoribbons by a facile and effective hydrothermal treatment whilst controlling condensation speeds of precursors in the solution along the $\langle 010 \rangle$, $\langle 100 \rangle$ and $\langle 001 \rangle$ directions. The prepared nanoribbon structure exhibited a high capacitance of 453 F/g. Figure 14 shows CV curves with a nearly rectangular shape, which indicates good conductivity and good charge propagation within the electrodes. Two pairs of obvious oxidation/reduction peaks (P1/P1' and P2/P2') and a pair of small oxidation/reduction peaks (P3/P3') were observed in the CV curves at five different scan rates. These CV curves displaying a nearly rectangular shape with three pairs of redox peaks, even at very high scan rates, indicate the supercapacitor features of fast charging and discharging.

Recently, 3D hybrid architectures composed of metal oxides and graphene have been shown to

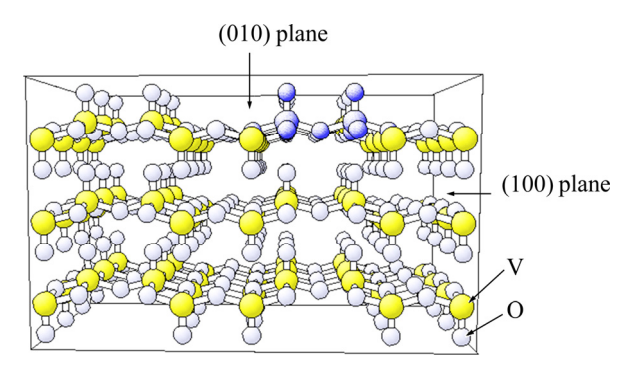


Fig. 13 Bulk lattice of V₂O₅ [84]

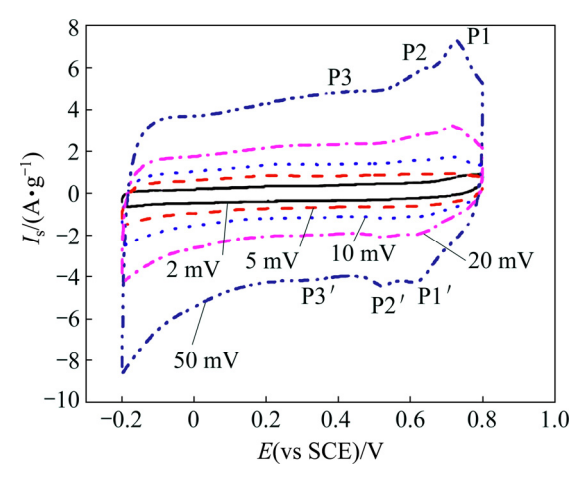


Fig. 14 CV curves of V₂O₅ at different scan rates [86]

potentially have better performance if a composite electrode possesses both the good rate performance of the carbon-based materials and the high specific capacitance of the metal oxides [87]. YE et al [88] synthesized a unique 3D architecture constructed by ultrathin single-crystalline V_2O_5 nanoribbons (V_2O_5 NRs) with reduced graphene oxide (rGO) layers via a simple hydrothermal synthesis and subsequent oxidation treatment (see Fig. 15).

The unique 3D V_2O_5 NR/rGO architecture exhibits a high capacitance of 437 F/g at a current density of 1 A/g, good stability and superior rate performances when applied as an electrode material for energy storage.

CHEN et al [89] developed a class of pseudocapacitive anode materials for asymmetric supercapacitors composed of interpenetrating networks of CNTs and V_2O_5 nanowires. The CNTs and nanowires were intimately intertwined into a hierarchically porous structure, enabling effective electrolyte access to the electrochemically active materials without limiting charge transport. The structure exhibited a high specific capacitance (>300 F/g) at a high current density (1 A/g) in aqueous electrolyte.

QU et al [90] uniformly grew PPy on the surface of $V_2O_5\,NRs$ using anionic dodecylbenzenesulfonate (DBS⁻) as a surfactant to overcome poor electronic conductivity and high dissolution in the liquid electrolyte (Fig. 16).

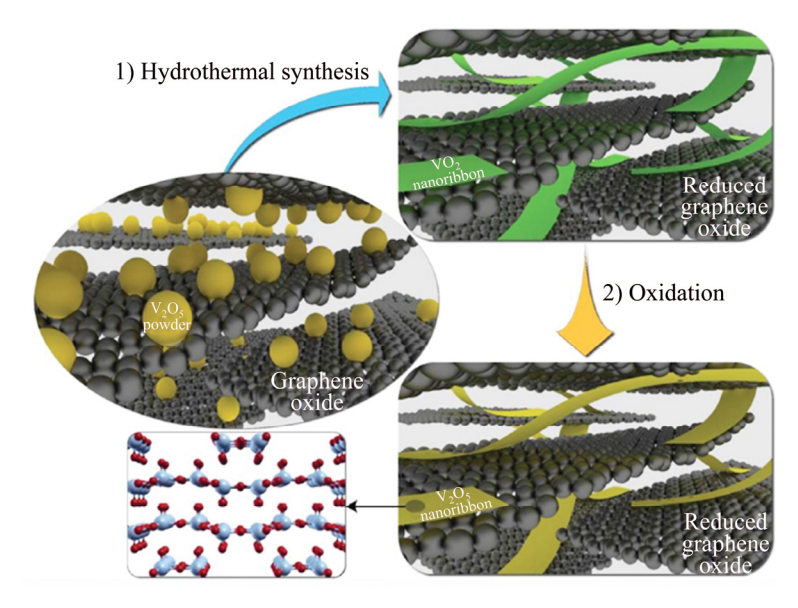


Fig. 15 Fabrication procedure of 3D V₂O₅ NR/rGO architecture [88]

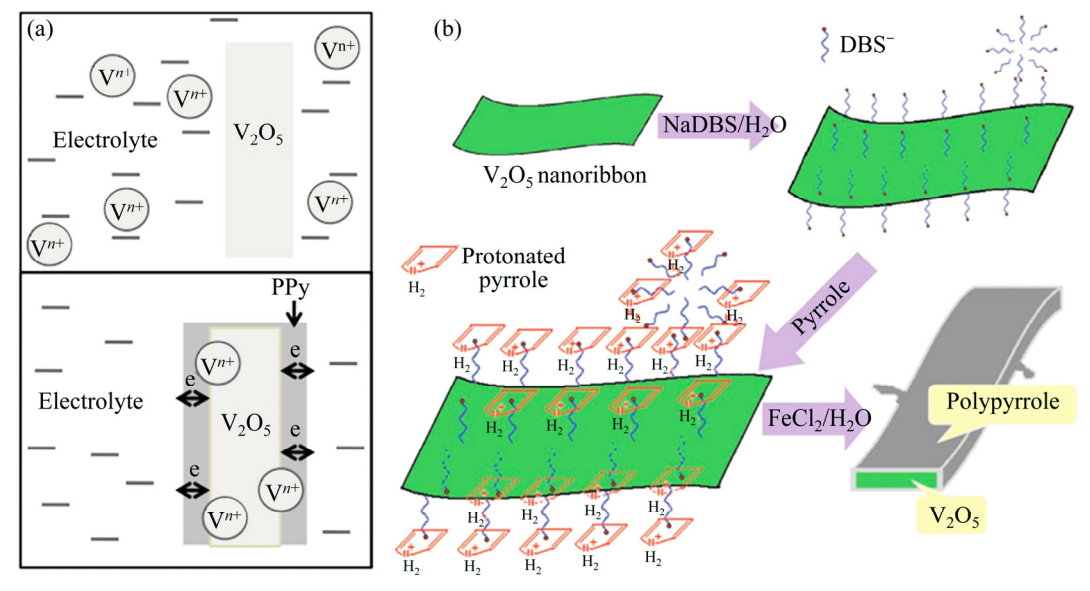


Fig. 16 PPy coating for facilitating electronic transport and preventing dissolution of vanadium in electrolyte (a) and schematic illustration of PPy growth on V_2O_5 NR surface (b) [90]

2.5 Cobalt oxides

Cobalt oxide has been paid significant attention for its importance in various scientific fields, such as solar selective absorbers, catalysts in the hydrocracking process of crude fuels, pigments for glasses and ceramics, catalysts for oxygen evolution and oxygen reduction reactions [91]. It has also newly used as an electrochemical material in supercapacitors. The theoretical specific capacitance of Co₃O₄ is 3560 F/g [92], much higher than for RuO₂, proving itself as a promising alternate to expensive RuO₂.

As a supercapacitor material, nanocrystalline Co₃O₄ can offer a large surface area, high conductivity, electrochemical stability and pseudocapacitive behavior,

which are beneficial for developing high energy and power density electrochemical capacitors. Although this oxide is customarily identified with its chemical formula Co_3O_4 , it is in fact, non-stoichiometric. Cobalt has less affinity for oxygen than iron has but more than nickel [93]. It has three well-known polymorphs: monoxide or cobaltous oxide (CoO), cobaltic oxide (Co2O₃) and cobaltosic oxide or cobalt cobaltite (Co₃O₄).

Figure 17 shows the CV curves of the Co_3O_4 product within a potential range of -0.4 to 0.55 V (vs Hg/HgO) at different scan rates of 5, 15 and 20 mV/s. It can be clearly seen that there are two strong distinct pairs of redox peaks during the anodic and cathodic sweeps. These redox peaks correspond to the conversion between

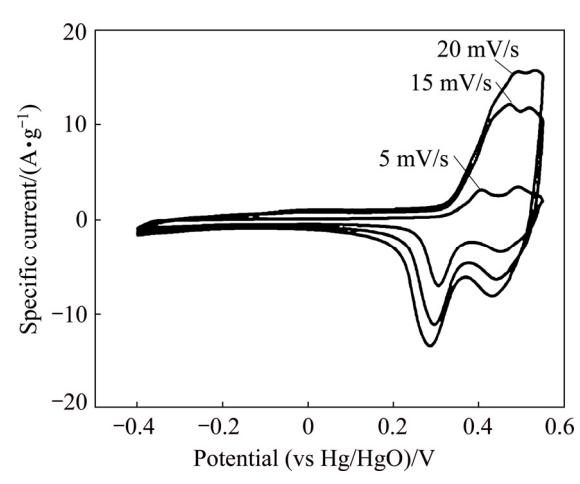


Fig. 17 CVs of Co₃O₄ product at different scan rates [94]

different cobalt oxidation states. In the case of oxidation, the two sequential reactions are described as follows [95]:

$$Co_3O_4+OH^-+H_2O \Longrightarrow 3CoOOH+e$$
 (5)

$$CoOOH+OH \rightleftharpoons CoO_2+H_2O+e \tag{6}$$

Recently, an emphasis has been given to the preparation of cobalt oxides using various physical and chemical techniques. Cobalt oxide thin films have been prepared by various methods, such as spray pyrolysis, sputtering, CVD, pulse laser deposition, sol-gel processes and electrodeposition on a variety of substrates [96,97]. Reports have proved that Co₃O₄ with a special microstructure and morphology possessed excellent electrochemical capacitive behavior. GAO et al [95] successfully prepared Co₃O₄ nanowire arrays on NF, which showed a maximum specific capacitance of 746 F/g measured at a current density of 5 mA/cm². Single crystal Co₃O₄ nanorods [98] were used as electroactive materials for supercapacitors and exhibited a high capacitance of 456 F/g. HU and LU [99] prepared aerogel-like mesoporous Co₃O₄ with an epoxide addition procedure, which exhibited a high specific capacitance of 600 F/g.

Although some improved properties have been achieved, the energy and power densities per unit area were relatively low. A 3D hybrid nanostructure, with short ion diffusion paths and an enlarged surface area, provides more efficient contact area between electrolyte ions and active materials for faradaic energy storage [100]. Carbon materials are considered as attractive electrode materials due to their superior electrical conductivity, high theoretical surface area and good electrochemical stability [86,101]. Carbon-based composites with metal oxides have been successfully synthesized for supercapacitors [102]. This could be a promising method to build better electrochemical materials.

DONG et al [103] reported a simple hydrothermal procedure which synthesized cobalt oxide (Co_3O_4) nanowires grown in-situ on 3D graphene foam using CVD (Fig. 18). The 3D graphene/ Co_3O_4 composite was used as the monolithic free-standing electrode for supercapacitor applications, it exhibited a high specific capacitance of ~1100 F/g at a current density of 10 A/g.

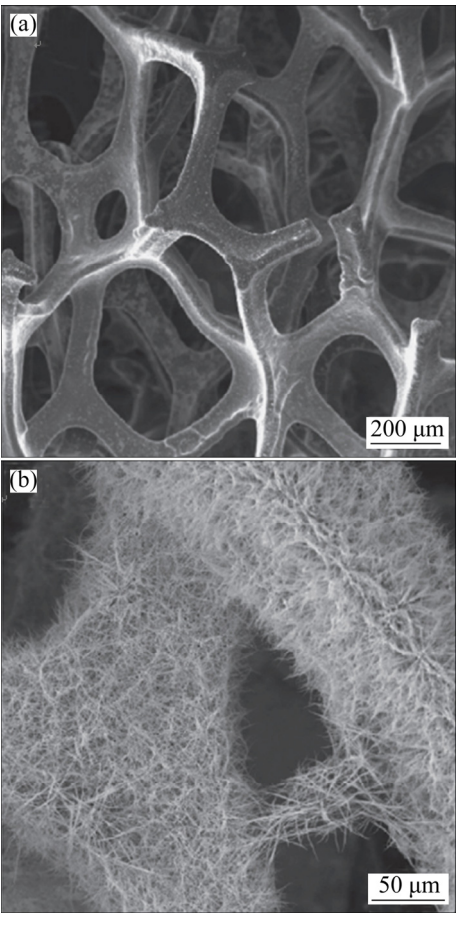


Fig. 18 SEM images of 3D graphene foam (a) and 3D graphene/ Co_3O_4 nanowire composite (b) [103]

WANG et al [104] presented the formation of porous NiCo oxide nanowires from single crystal nickel cobalt bimetallic carbonate hydroxide nanowires for supercapacitor applications. The porous nickel cobalt oxide ($Ni_xCo_{3-x}O_4$) nanowire array is formed by the heat treatment of nickel cobalt bimetallic carbonate hydroxide nanowires on NF for the assembly of supercapacitors, showing a high specific capacitance of 1479 F/g at 1 A/g.

Cobalt hydroxide (Co(OH)₂) with layered structure, which can result in high utilization of the electrode material, exhibits higher capacitance than cobalt oxides [105].

Figure 19 shows the CV curves of the $Co(OH)_2$ product. For the $Co(OH)_2$ electrode material, two plausible reactions could occur as quasi-reversible redox processes during the potential sweep of the film electrode. The mechanisms of electric energy storage for

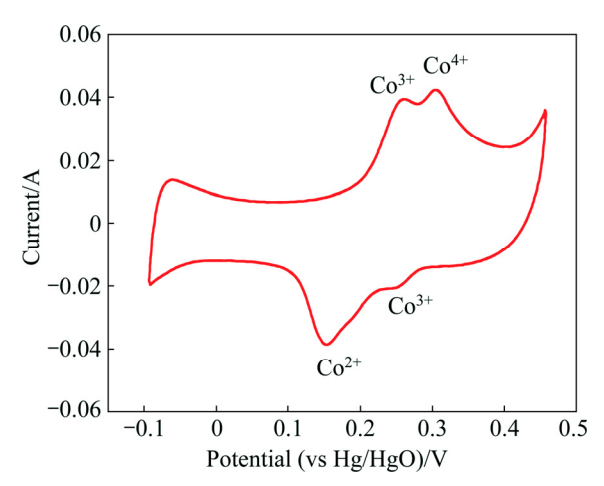


Fig. 19 CV curves of α -Co(OH)₂ at 10 mV/s [106]

the pseudocapacitor are proposed as follows:

$$Co(OH)_2 + OH - CoOOH + H_2O + e$$
 (7)

$$CoOOH+OH \xrightarrow{} CoO_2+H_2O+e$$
 (8)

ZHOU [107] successfully synthesized ordered mesoporous cobalt hydroxide films on substrates. Various electrochemical test results show that the ordered mesoporous cobalt hydroxide film on foamed Ni mesh has a much high specific capacitance.

2.6 Iridium oxides

In 1977, HORKANS et al [108] reported that an IrO_2 multicrystalline electrode showed distinct CV current peaks in 1 mol/L H_2SO_4 , and it achieved approximately equal anodic and cathodic charges. Rutile IrO_2 has metal-like conductivity, excellent chemical stability and versatile oxidation states, and shows promising application in pseudocapacitive energy storage and electrochemical catalysis (i.e. chlorine and oxygen evolution) [109]. For example, LIU et al [110] investigated the supercapacitive properties of IrO_2 thin films prepared by radio frequency magnetron sputtering from room temperature to 300 °C. The amorphous film sputtered at room temperature exhibited the highest value of 293 F/g at 5 mV/s and retained 271 F/g after 1000 cycles.

The inhibitive price of IrO₂ has provoked much interest in compositing it with other oxides or carbon materials for practical use. GRUPIONI et al [111] reported that, compared with IrO₂ annealed at 450 °C exhibiting 21 F/g, IrO₂ in Ir_{0.3}Mn_{0.7}O₂ showed a significant increase to 410 F/g, and 550 F/g annealed at 400 °C, due to the promoted Ir active surface sites. SHAO et al [112] investigated the electrochemical performance of a binary oxide of 70% IrO₂–30%ZrO₂ coating annealed at 340–400 °C. It was demonstrated that 360 °C is the optimal annealing temperature, which produced IrO₂ nanocrystals (1–2 nm in diameter) embedded in an amorphous matrix with the highest

specific capacitance of 182.7 F/g. CHEN et al [113] grew IrO_2 nanocrystals on vertically aligned CNTs, revealing 3590 $\mu F/cm^2$, which was apparently better than 580 $\mu F/cm^2$ for just CNTs. SHIH et al [114] first grew CNTs with a honeycomb arrangement based on graphene via a CVD procedure, then decorated them with sheet-like shape IrO_2 by RFMS. The composite exhibited 139.1 F/g at 10 mV/s and 129.4 F/g after 1000 cycles at 1 mA, which showed higher specific capacitance and a more stable structure compared with $IrO_2/CNT/graphene$ with the bundle arrangement.

3 Transition metal nitrides

Transition metal nitrides, such as TiN, VN, WN, MoNx, Nb4N5, TaN and CrN, can be used as pseudocapacitor electrode materials. In 1985, VOLPE et al [115] found that a temperature-programmed reaction between MoO₃ or WO₃ with NH₃ could produce Mo₂N and W₂N powders with specific surface areas as high as 220 and 91 m²/g, respectively, thereby providing a new direction for transition metal nitride research in the field of catalysis. As a result of such research, a broad range of application prospects for transition metal nitrides have been discovered. They have excellent electrochemical performance, good electrochemical stability and are stable in aqueous electrolyte. Moreover, the raw materials are low cost, meaning that transition metal nitrides have become a hot topic in the field of supercapacitor electrode materials.

The synthesis of transition metal nitrides is usually divided into physical synthesis and chemical synthesis [116]. Physical synthesis mainly includes ball milling, physical vapor deposition and laser vaporization, which can only composite several transition metal nitrides, such as TiN and CrN. Metal oxides or other metal precursors can be used as raw materials, and ammonia gas or nitrogen can be used as the nitrogen source at high temperatures (800–2000 °C) [117], which can be widely used in the preparation of nitrides.

These nitrides exhibit similar electrochemical behavior to that of RuO_2 and show capacitive behavior at high scan rates due to their high electronic conductivity and fast reversible redox process. Among all the transition metal nitrides, only VN, TiN and MoN_x have shown relatively good capacitance [118]. Currently, VN, TiN and its complex have a wide range of applications in supercapacitors. The theoretical specific capacitance is calculated by Eq. (9) (n is the change of valence states, F is the faraday constant, V is voltage window and M is relative molecular mass), and the calculated results are shown in Table 2.

$$c = \frac{nF}{VM} \tag{9}$$

Table 2 Relevant data for transition metal nitrides

Transition metal nitride	Relative molecular mass	Change of valence state	Voltage window/V
TiN	62	1	0.6 (-0.3 to 0.3)
VN	65	1	1.2 (-1.2 to 0)
MoN	110	1	0.7 (0-0.7)
Nb_4N_5	442	2	0.6 (0-0.6)
RuN	115	2	1 (-0.5 to 0.5)
CrN	66	1	3 (0-3)
CoN	73	1	3 (0-3)

3.1 Titanium nitrides

As one of the most common nitrides, TiN and its complex are widely used as pseudocapacitor electrode materials. Though TiN has a minor capacity, its electronic conductivity is proved to be excellent, and is usually used as a current collector. LI et al [119] prepared mesoporous TiN through a solvothermal reaction and a short-time nitridation process (Fig. 20(a)). The surface area of TiN reached 50.6 m²/g and the pore sizes are in the range of 2–4 nm.

DONG et al [120] fabricated mesoporous TiN spheres through a facile template-free strategy. Under an ammonia atmosphere, mesoporous TiO₂ spheres are directly converted into mesoporous TiN spheres with the addition of cyanamide to retain the original morphology. The energy density of TiN can reach 45 W·h/kg at a power density of 150 W/kg, and still remains 12.3 W·h/kg at a power density of 3 kW/kg, which shows that mesoporous TiN and its complex have great potential. By modifying and loading, its performance can be further improved.

The TiN nanoarray substrates can provide a large surface area, fast electron transport and can enhance structural stability. XIE et al [121] prepared TiN nanoarrays with a short nanotube and long nanopore structure by anodizing ultra-thin titanium foil in an

ethylene glycol solution containing ammonium fluoride, calcining in air and nitriding in ammonia. The specific capacitance of the TiN nanopore array reached an extraordinarily high level of up to 99.7 mF/cm² at a current density of 0.2 mA/cm², which is a significant improvement on the TiN nanotube array. At a high current density of 5 mA/cm², the TiN nanoarray supercapacitor maintained a specific power of 8.15 mW/cm² (204 mW/cm³) and a specific energy of 35.98 (mW·s)/cm² (900 (mW·s)/cm³). The power and energy densities of the flexible TiN nanoarray supercapacitor are higher than those of the traditional activated carbon supercapacitor.

By compounding with other electrochemical materials, the performance of TiN has been improved. PENG et al [122,123] successfully fabricated PANI or MoO_x on the outer and inner surfaces of TiN nanotubes to form an interpenetrating 3D network, forming PANI/TiN or MoO_x /TiN NTA hybrid nanostructures (Fig. 21(a)).

Coaxial PANI/TiN/PANI nanotube arrays were fabricated by electrochemical polymerization of PANI on nanoporous TiN nanotube arrays. They exhibit a high specific capacitance of 242 mF/cm², excellent rate capability with the capacitance remaining at 69% when the current density increases from 0.2 to 10 mA/cm², and a long cycling life with less than 0.005% decay per cycle.

Porous dual-layered MoO_x NTAs with highly conductive TiN cores were fabricated by depositing MoO_x on porous TiN. The coaxial MoO_x/TiN/MoO_xNTA electrode shows a high specific capacitance of 97 mF/cm² (323 F/g) at a current density of 1 mA/cm², and still retains 60% capacitance when the current density is increased 20 times.

MnO₂-TiN nanotube hybrids were prepared by loading electroactive MnO₂ into well-aligned TiN nanotubes through a cyclic voltammetry electrodeposition process, which was directly supported on ultra-thin

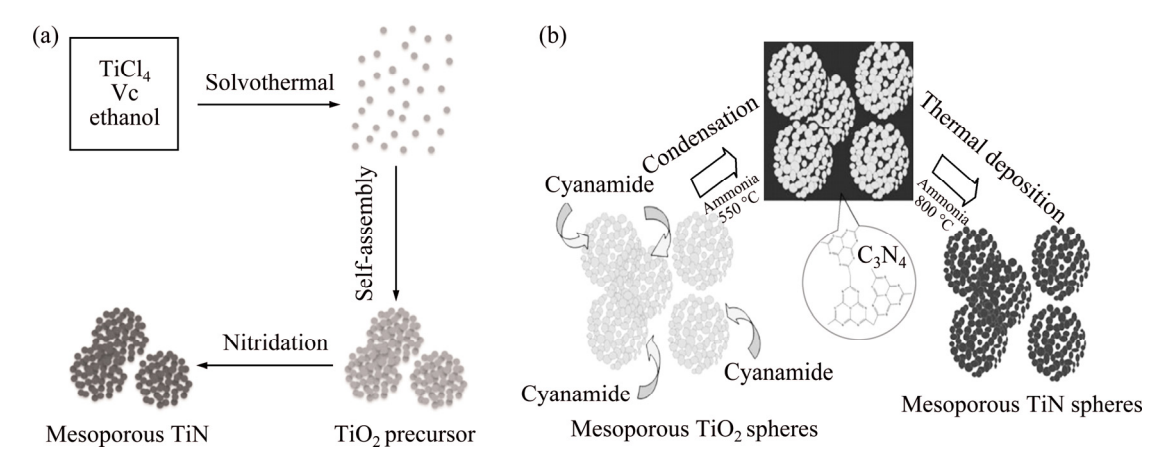


Fig. 20 Schematic illustration for preparation of mesoporous TiN [119]

and supple titanium foil. Due to the coaxial heterogeneous structure, the specific capacitance of MnO_2 –TiN was determined to be 853.3 F/g (213.2 mF/cm²) at a current density of 1 A/g (0.25 mA/cm²) [124].

SHANG et al [125] prepared $Ni_xCo_{2x}(OH)_{6x}/TiN$ by directly depositing $Ni_xCo_{2x}(OH)_{6x}/TiN$ into a self-standing TiN NTA grid monolithic (Fig. 21(b)). It exhibits superior pseudocapacitive performance due to the coaxial nanostructure. The specific capacitance reaches 2543 F/g at 5 mV/s, the rate performance reaches 660 F/g at 500 mV/s, and a loss of only about 6.25% capacitance after 5000 cycles is observed, which are much better than for the $NiCo_2O_4/TiN$ electrode.

LU et al [126] produced TiC@C by coating a uniform and ultrathin carbon shell to the TiN nanowire surface through hydrothermal methods, followed by annealing at 800 °C in a N_2 gas atmosphere (Fig. 22).

3.2 Vanadium nitrides

Among the various options, nanocrystalline VN, which has been reported to deliver a specific capacitance of up to 1340 F/g at a scan rate of 2 mV/s, and still maintain 554 F/g at a higher scan rate of 100 mV/s [127], is clearly one of the most promising candidates for pseudocapacitors. Nanocrystalline VN has been synthesized by a two-step ammonolysis reaction of VCl₄

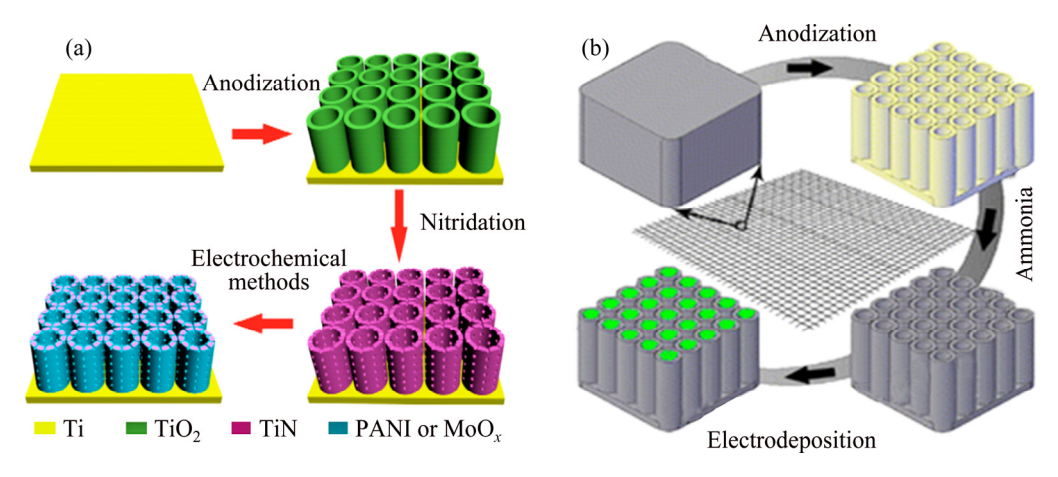


Fig. 21 Fabrication process of TiN-based composite nanostructures (a) and Ni_xCo_{2x}(OH)_{6x}/TiN (b) [120]

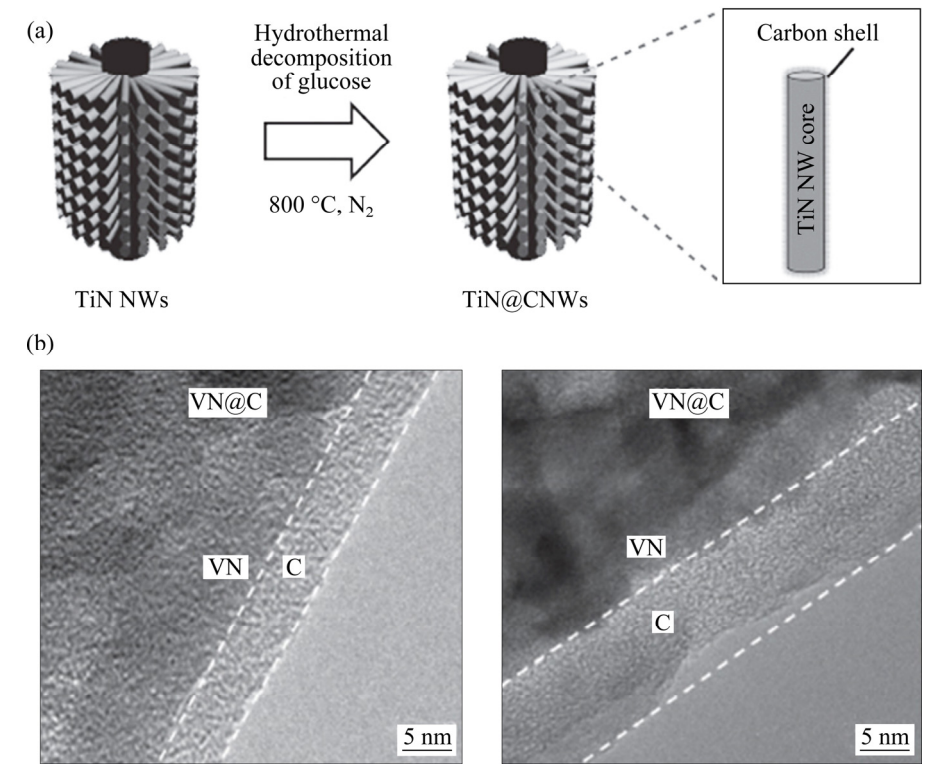


Fig. 22 Schematic illustration (a) of process of applying carbon shell to TiN NWs and HRTEM images of VN@C (b) and VN@2C NWs (c) [126]

in anhydrous chloroform. Such a high capacitance is obtained due to the pseudocapacitance contribution from the low specific surface area of nitride (38 m²/g) [128].

ZHOU et al [129] found another way to produce VN powder by calcining V_2O_5 xerogel in a furnace under an anhydrous NH_3 atmosphere at 400 °C. The specific capacitance of VN reached 161 F/g at 30 mV/s. Furthermore, 70% specific capacitance remained when the scan rate was increased from 30 to 300 mV/s. GLUSHENKOV et al [130] used the same method to produce VN and capacitance of 186 F/g was obtained at 1 A/g. The large volume of pores in VN is represented by the range of 15–110 nm.

VN was reported to exhibit an excellent electrochemical performance, especially with regards to specific capacity. However, it also exhibits poor electronic conductivity, resulting in its limited rate capability. To improve the performance of VN, the fabrication of hybrid devices based on VN has become a new and promising strategy. SU et al [131] prepared VN-MWCNT by annealing V_2O_5 mixed with pre-treated CNTs at 800 °C in a N_2 gas atmosphere for 3 h. The

results indicate that VN-MWCNT electrodes exhibit good capacitance retention, good cycling stability and a high specific capacitance of 160 F/g at a scan rate of 2 mV/s.

DONG et al [132] combined VN and TiN to seek both faster electronic transportation and excellent storage performance, since both VN and TiN feature the same diffraction patterns and similar cell parameters. TiN/VN core-shell composites were prepared by a two-step strategy involving coating the commercial TiN nanoparticles with V_2O_5 sols followed by ammonia reduction (Fig. 23). The highest specific capacitance of 170 F/g was obtained at a scan rate of 2 mV/s and a promising rate capacity performance is maintained at higher voltage sweep rates.

ZHANG et al [133] synthesized 3D electrochemically supercapacitive arrays, the multiwalled carbon nanotubes covered by nanocrystalline VN were firmly anchored to glassy carbon or Inconel electrodes (Fig. 24). These nanostructures demonstrate a respectable specific capacitance of 289 F/g at a scan rate of 20 mV/s, and at least 80% capacitance still remains at

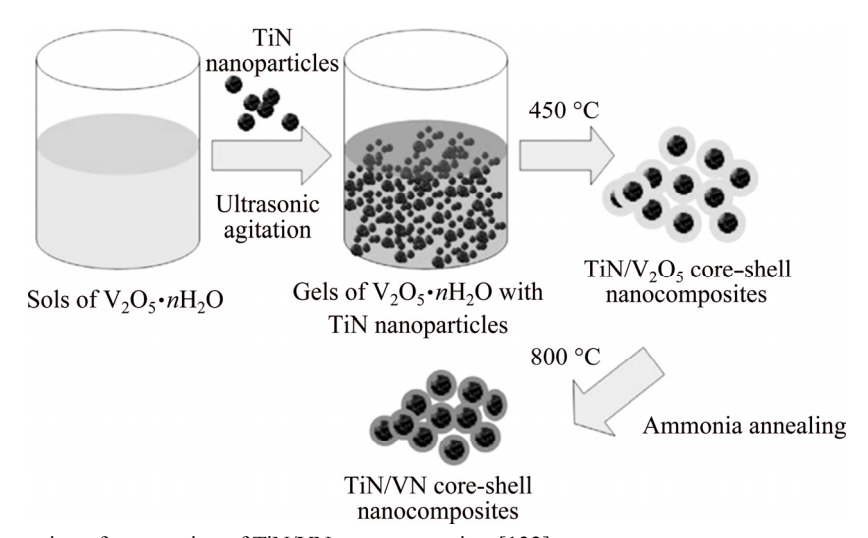


Fig. 23 Schematic illustration of preparation of TiN/VN nanocomposites [132]

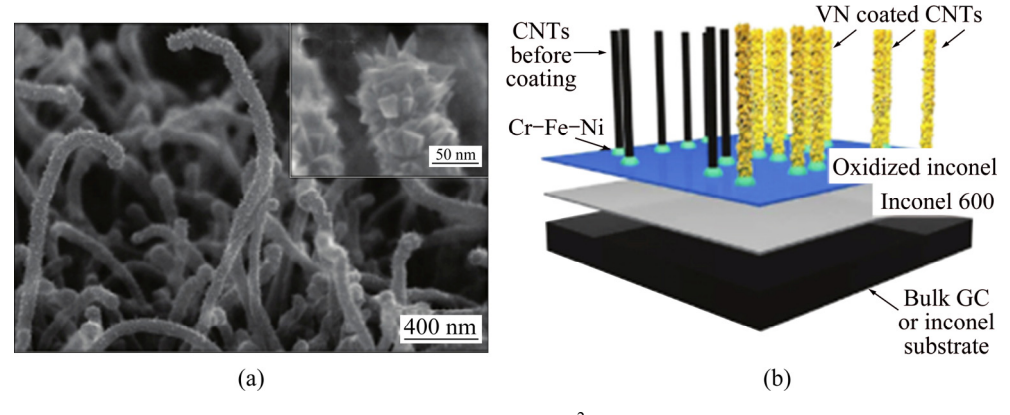


Fig. 24 SEM images of VN/CNT/Inconel/GC (VN mass = 0.037 mg/cm²) (a) and schematic illustration of preparation of ultimate morphology of VN/CNT 3D array (b) [133]

20 mV/s, which is the highest rate capability reported for VN materials. Analysis of the post-electrochemically cycled samples indicates negligible changes occurring in the VN nanocrystallite morphology, but a modification in the structure of the oxidized surface.

3.3 Molybdenum nitrides

In 1995, FINELLO et al [134] applied Mo₂N/MoN films, produced by ammonolysis of MoO₃, to supercapacitor electrode materials for the first time. These compounds are stable in aqueous H₂SO₄. Their redox behavior is similar to that of RuO₂ [135], but their capability was limited due to their smaller electrochemical window of ~0.7 V compared with the ~1.4 V for RuO₂. The most studied nitrides of molybdenum are the rocksalt-type γ -MoN_x (x=0.39–0.54), also known as γ -Mo₂N [136]. There are another three types of molybdenum nitrides, including δ_1 -Mo₂N, δ_2 -Mo₂N and δ_3 -Mo₂N [137].

IMRAN et al [138] produced cubic γ-Mo₂N and hexagonal δ_1 -MoN through the reactions of MoCl₅ or Mo(NMe₂)₄ with ammonia at different temperatures and reaction times (Table 3). Most molybdenum nitrides show relatively smaller surface areas and capacitances, while their redox capacitance are high enough to be used in charge storage devices. The highest capacitances can reach 275 F/g at 2 mV/s, indicating that it can be used as a pseudocapacitor electrode. A MoN/nitrogen-doped graphene sheets composite delivers specific capacitance of 422 F/g at the current density of 0.05 A/g, and can maintain more than 80% after 900 cycles [139]. The energy density remains as high as 32.5 W h/kg when the power density is 3000 W/kg. However, due to its lower working voltage window in water electrolysis systems and low density, its performance cannot be fully utilized.

3.4 Niobium nitride and other transition metal nitrides

Some niobium nitrides, including Nb_2N , Nb_4N_3 and NbN, are famous for their excellent superconducting properties [140]. Recently, CUI et al [141] found

Table 3 Refined parameters and analytical data for molybdenum nitride samples produced by pyrolysis of imide precursor [138]

Temperature/ °C	Heating time/h	Crystallite size/nm Composition		Surface area/ (m ² ·g ⁻¹)
1000	2	14 or 28	$MoN_{0.58}$	2
900	2	4.4 or 14	$MoN_{0.80}$	2.8
800	2	8.8	$MoN_{0.84}C_{0.03} \\$	3.1
700	2	6	$MoN_{0.81}C_{0.03} \\$	4.9
600	2	4	$MoN_{0.83}C_{0.05}$	9.8
500	2	4	$MoN_{0.74}C_{0.08}H_{0.5}$	9
500	48	4	$MoN_{1.02}$	8

nitrogen-rich Nb_4N_5 phases that comprise high valence Nb^{5+} ions and could be a new high-performance electrode material for supercapacitors. Nb_4N_5 is proved to have a capacitance of 225.8 mF/cm² for the first time, and Nb_4N_5 nanochannels electrode remains 70.9% capacitance after 2000 cycles, moreover, it shows nearly 100% capacitance retention after 2000 CV cycles when coating an ultrathin carbon to the surface (Fig. 25). This new advanced material can also be used as a support to deposit other electrochemical active materials and is expected to be useful for industry applications.

There are many other transition metal nitrides that can be regarded as excellent pseudocapacitor materials, such as chrominum nitride, cobalt nitride, ruthenium nitride and so on. DAS et al [142] prepared CrN and CoN nanoparticles of particle size 20–30 nm from Cr₂O₃ and Co₃O₄ at relatively low temperature under a NH₃+N₂ atmosphere. The specific capacitances of CrN/AC and CoN/AC are, respectively, 75 and 37 F/g at a current density of 30 mA/g. CrN/AC showed almost stable performance, while the capacitance of CoN/AC fade quickly. The energy densities of CrN/AC and CoN/AC calculated from galvanostatic cycling were 30 and 44 W·h/kg, respectively. BOUHTIYYA et al [143] use sputtered ruthenium nitride thin films as electrode material, and the capacitance shows 37 F/g at a scan rate

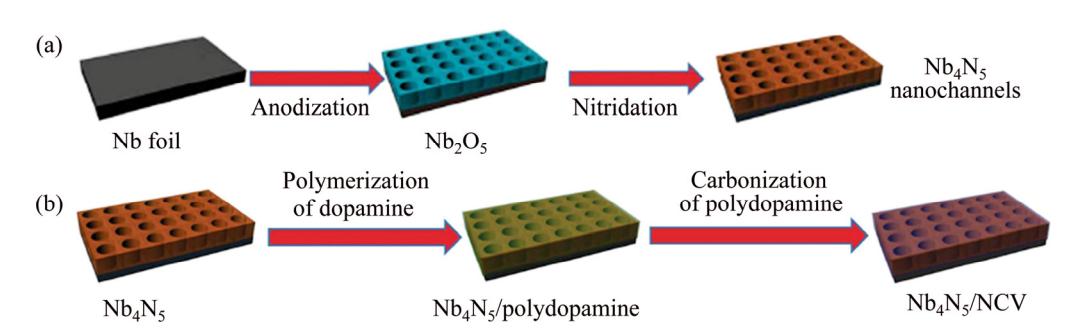


Fig. 25 Schematic illustration of fabrication of Nb_4N_5 nanochannels (a) and N-doped carbon coating on surface of Nb_4N_5 nanochannels (b) [141]

of 200 mV/s. Those preparation methods can be tried to open up other new nitrides or hydroxide systems, such as Ti, W, Zr and Ta.

4 Summary and outlook

Several pseudocapacitor electrode materials, including transition metal oxides and nitrides, have been discussed along with the fabrication challenges involved with increasing energy density.

Different from EDLCs, whose performance is limited low-capacitance carbon materials, pseudocapacitors have much higher energy density and wide application prospects. Since protons, electrons and ions transmission are required for an efficient pseudocapacitance, exploitation appropriate microstructure and morphology control for transmission channels is necessary. Nowadays, nanofabrication technology enabled the development has nanoarchitectured electrodes, where the oxide or nitride component was deposited in various forms, such as nanoflowers, nanoflakes, nanorods, nanosheets, nanoparticles, etc. The specific capacitance of various pseudocapacitor materials or its composites and carbon materials are shown in Fig. 26. Metal oxides and nitrides have much higher practical specific capacitance than those of carbon and conducting polymers. Research into transition metal oxides is relatively mature, while for transition metal nitrides, their potential application has yet to be exploited.

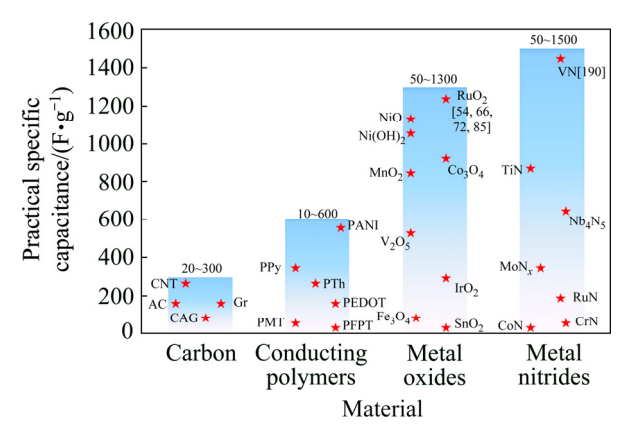


Fig. 26 Specific capacitance of various pseudocapacitor materials (or their composites) and carbon materials

To improve the relatively low conductivity and cycling stability, several electrochemical active materials are composited with transition metal oxides and nitrides. Taking into account the mechanism involving the surface, as well as the bulk of metal oxides or nitrides, the diffusion of protons accompanying the charge transfer must be ensured by the presence of mesoporous structure. Building a hierarchical structure of the

composite could develop the specific surface area of oxides or nitrides maximally. Carbon materials are excellent accessible candidates with relatively high specific surface areas to act as perfect supports for such pseudocapacitive materials. Also, well-distributed carbon in the composite can greatly enhance the low conductivity of transition metal oxides and nitrides. However, compounding carbon with metal oxides or nitrides still requires considerable effort to avoid adversely affecting the overall performance of the composite. Multitudinous carbon materials provide plenty of possibilities. It is still difficult to monitor the characteristics, surface such as area, size/distribution, density and conductivity, to optimize composite properties, as many of these properties can be mutually exclusive.

The application of such a redox-active reaction presents a new attractive trend in capacitor development to increase both the energy density and the power density. Pseudocapacitor electrode materials have shown excellent performance and great potential. As research goes further, lighter, smaller, higher energy and more stable electrochemical pseudocapacitors will be realized in the near future, which will play an important role in the field of energy storage and conversion.

References

- [1] OMAR N, DAOWD M, HEGAZY O, SAKKA M A, COOSEMANS T, BOSSCHE P V D, MIERLO J V. Assessment of lithium-ion capacitor for using in battery electric vehicle and hybrid electric vehicle applications [J]. Electrochimica Acta, 2012, 86(4): 305–315.
- [2] BÉGUIN F, PRESSER V, BALDUCCI A, FRACKOWIAK E. Carbons and electrolytes for advanced supercapacitors [J]. Advanced Materials, 2014, 26(14): 2219–2251.
- [3] ZHANG W, MA C, FANG J, CHENG J, ZHANG X, DONG S, ZHANG L. Asymmetric electrochemical capacitors with high energy and power density based on graphene/CoAl-LDH and activated carbon electrodes [J]. Rsc Advances, 2013, 3(7): 2483–2490.
- [4] XIE K, QIN X, WANG X, WANG Y, TAO H, WU Q, YANG L, HU Z. Carbon nanocages as supercapacitor electrode materials [J]. Advanced Materials, 2012, 24(3): 347–352.
- [5] OKASHY S, NOKED M, ZIMRIN T, AURBACH D. The study of activated carbon/CNT/MoO₃ electrodes for aqueous pseudocapacitors [J]. Journal of the Electrochemical Society, 2013, 9(160): A1489–A1496.
- [6] ZHANG K, ZHANG L L, ZHAO X S, WU J. Graphene/polyaniline nanofiber composites as supercapacitor electrodes [J]. Chemistry of Materials, 2010, 22(4): 1392–1401.
- [7] GUPTA V, MIURA N. High performance electrochemical supercapacitor from electrochemically synthesized nanostructured polyaniline [J]. Materials Letters, 2006, 60(12): 1466–1469.
- [8] AMBADE R B, AMBADE S B, SHRESTHA N K, NAH Y C, HAN S H, LEE W, LEE S H. Polythiophene infiltrated TiO₂ nanotubes as high-performance supercapacitor electrodes [J]. Chemical Communications, 2013, 49(23): 2308–2310.
- [9] PATIL B H, PATIL S J, LOKHANDE C D. Electrochemical

- characterization of chemically synthesized polythiophene thin films: Performance of asymmetric supercapacitor device [J]. Electroanalysis, 2014, 26(9): 2023–2032.
- [10] LIU T, FINN L, YU M, WANG H, ZHAI T, LU X, TONG Y, LI Y. Polyaniline and polypyrrole pseudocapacitor electrodes with excellent cycling stability [J]. Nano Letters, 2014, 14(5): 2522–2527.
- [11] DETTLAFF A, WILAMOWSKA M. Electrochemical synthesis and characterization of nanocomposites based on poly(3,4-ethylenedioxythiophene) and functionalized carbon nanotubes [J]. Synthetic Metals, 2016, 2(12): 31–43.
- [12] NIU J, CONWAY B E, PELL W G. Comparative studies of self-discharge by potential decay and float-current measurements at C double-layer capacitor and battery electrodes [J]. Journal of Power Sources, 2004, 135(1–2): 332–343.
- [13] JUREWICZ K, FRACKOWIAK E, BÉGUIN F. Enhancement of reversible hydrogen capacity into activated carbon through water electrolysis [J]. Electrochemical and Solid-State Letters, 2001, 3(4): A27-A30.
- [14] SHI F, LI L, WANG X L, GU C D, TU J P. Metal oxide/hydroxide-based materials for supercapacitors [J]. Rsc Advances, 2014, 4(79): 41910–41921
- [15] DENNIS ANTIOHOS M R J C, RAZAL J M. Carbon nanotubes for energy applications [J]. Nanotechnology and Nanomaterials, 2013, 7(19): 65–73.
- [16] WANG C, XU J, YUEN M F, ZHANG J, LI Y, CHEN X, ZHANG W. Hierarchical composite electrodes of nickel oxide nanoflake 3D graphene for high-performance pseudocapacitors [J]. Advanced Functional Materials, 2014, 24(40): 6372–6380.
- [17] TRASATTI S, BUZZANCA G. Ruthenium dioxide: A new interesting electrode material, solid state structure and electrochemical behaviour [J]. Journal of Electroanalytical Chemistry, 1971, 2(29): A1–A5.
- [18] ZHENG J. A new charge storage mechanism for electrochemical capacitors and charge storage density vs. crystalline structure of metal oxides [J]. Mrs Online Proceeding Library, 2011, 1(393): 13-20.
- [19] LENG X, ZOU J, XIONG X, HE H. Electrochemical capacitive behavior of RuO₂/graphene composites prepared under various precipitation conditions [J]. Journal of Alloys & Compounds, 2015, 6(53): 577–584.
- [20] KIM I H, KIM K B. Electrochemical characterization of hydrous ruthenium oxide thin-film electrodes for electrochemical capacitor applications [J]. Journal of the Electrochemical Society, 2006, 153(2): A383-A389.
- [21] CHANG K H, HU C C, CHANG K H, HU C C. Hydrothermal synthesis of hydrous crystalline RuO₂ nanoparticles for supercapacitors [J]. Electrochemical & Solid State Letters, 2004, 7(12): 156–164.
- [22] DESHMUKH P R, PUSAWALE S N, BULAKHE R N, LOKHANDE C D. Supercapacitive performance of hydrous ruthenium oxide ($RuO_2 \cdot nH_2O$) thin films synthesized by chemical route at low temperature [J]. Bulletin of Materials Science, 2013, 36(7): 1171–1176.
- [23] CREUTZ C, AI E. Charge transfer on the nanoscale: Current status [J]. ChemInform, 2003, 34(38): 6668–6697.
- [24] HU C C, CHEN W C, CHANG K H, HU C C, CHEN W C, CHANG K H. How to achieve maximum utilization of hydrous ruthenium oxide for supercapacitors [J]. Journal of the Electrochemical Society, 2004, 151(2): A281–A290.
- [25] KURATANI K, KIYOBAYASHI T, KURIYAMA N. Influence of the mesoporous structure on capacitance of the RuO₂ electrode [J].

- Journal of Power Sources, 2009, 189(2): 1284-1291.
- [26] WU X, ZENG Y, GAO H, SU J, LIU J, ZHU Z. Template synthesis of hollow fusiform RuO₂·xH₂O nanostructure and its supercapacitor performance [J]. Journal of Materials Chemistry A, 2012, 1(3): 469–472.
- [27] ZHANG J, MA J, ZHANG L L, GUO P, JIANG J, ZHAO X S. Template synthesis of tubular ruthenium oxides for supercapacitor applications [J]. Journal of Physical Chemistry C, 2010, 32(114): 13608-13613.
- [28] LIN K M, CHANG K H, HU C C, LI Y Y. Mesoporous RuO₂ for the next generation supercapacitors with an ultrahigh power density [J]. Electrochimica Acta, 2009, 54(19): 4574–4581.
- [29] JEONG M G, KAI Z, CHEREVKO S, KIM W J, CHUNG C H. Facile preparation of three-dimensional porous hydrous ruthenium oxide electrode for supercapacitors [J]. Journal of Power Sources, 2013, 4(244): 806–811.
- [30] SUGIMOTO W, IWATA H, MURAKAMI Y, TAKASU Y. Electrochemical capacitor behavior of layered ruthenic acid hydrate [J]. Journal of the Electrochemical Society, 2004, 8 (151): A1181–A1187.
- [31] SUGIMOTO W, IWATA H, YASUNAGA Y, MURAKAMI Y, TAKASU Y. Preparation of ruthenic acid nanosheets and utilization of its interlayer surface for electrochemical energy storage [J]. Angewandte Chemie, 2003, 42(34): 4092–4096.
- [32] HYUN T S, TULLER H L, YOUN D Y, KIM H G, KIM I D. Facile synthesis and electrochemical properties of RuO₂ nanofibers with ionically conducting hydrous layer [J]. Journal of Materials Chemistry, 2010, 20(20): 9172–9179.
- [33] DIAH S, DAHSHYANG T, HUANG Y S, ALEXANDRU KOROTCOV A, CHUNG W H. Structures and electrochemical capacitive properties of RuO₂ vertical nanorods encased in hydrous RuO₂ [J]. Journal of Physical Chemistry C, 2007, 111(26): 9530–9537.
- [34] PONROUCH A, GARBARINO S, BERTIN E, GUAY D. Ultra high capacitance values of Pt@RuO₂ core–shell nanotubular electrodes for microsupercapacitor applications [J]. Journal of Power Sources, 2013, 221(1): 228–231.
- [35] RYU I, YANG M H, KWON H, PARK H K, DO Y R, SANG B L, YIM S. Coaxial RuO₂-ITO nanopillars for transparent supercapacitor application [J]. Langmuir, 2014, 30(6): 1704–1709.
- [36] LIN C, RITTER J A, POPOV B N. Development of carbon-metal oxide supercapacitors from sol-gel derived carbon-ruthenium xerogels [J]. Journal of the Electrochemical Society, 1999, 146(9): 3155-3160.
- [37] MILLER J M A, DUNN B. Morphology and electrochemistry of ruthenium/carbon aerogel nanostructures [J]. Langmuir, 1999, 3(15): 799–806
- [38] FANG H T, LIU M, WANG D W, REN X H, SUN X. Fabrication and supercapacitive properties of a thick electrode of carbon nanotube–RuO₂ core–shell hybrid material with a high RuO₂ loading [J]. Nano Energy, 2013, 2(6): 1232–1241.
- [39] ZHOU Z, ZHU Y, WU Z, LU F, JING M, JI X. Amorphous RuO₂ coated on carbon spheres as excellent electrode materials for supercapacitors [J]. Rsc Advances, 2014, 4(14): 6927–6932.
- [40] AN G H, AHN H J. Surface modification of RuO₂ nanoparticles– carbon nanofiber composites for electrochemical capacitors [J]. Journal of Electroanalytical Chemistry, 2015, 7(44): 32–36.
- [41] HSIEH T F, CHUANG C C, CHEN W J, HUANG J H, CHEN W T, SHU C M. Hydrous ruthenium dioxide/multi-walled carbonnanotube/titanium electrodes for supercapacitors [J]. Carbon, 2012, 50(5): 1740–1747.

- [42] WANG P, XU Y, LIU H, CHEN Y, YANG J, TAN Q. Carbon/carbon nanotube-supported RuO₂ nanoparticles with a hollow interior as excellent electrode materials for supercapacitors [J]. Nano Energy, 2015, 15(18):116–124.
- [43] ZHU Y, JI X, PAN C, SUN Q, SONG W, FANG L, CHEN Q, BANKS C E. A carbon quantum dot decorated RuO₂ network: Outstanding supercapacitances under ultrafast charge and discharge [J]. Energy & Environmental Science, 2013, 6(12): 3665–3675.
- [44] WU Z S, WANG D W, REN W, ZHAO J, ZHOU G, LI F, CHENG H M. Anchoring hydrous RuO₂ on graphene sheets for highperformance electrochemical capacitors [J]. Advanced Functional Materials, 2010, 20(20): 3595–3602.
- [45] DINH T M, ACHOUR A, VIZIREANU S, DINESCU G, NISTOR L, ARMSTRONG K, GUAY D, PECH D. Hydrous RuO₂/carbon nanowalls hierarchical structures for all-solid-state ultrahigh-energydensity micro-supercapacitors [J]. Nano Energy, 2014, 10(10): 288–294.
- [46] WANG W, GUO S, LEE L, AHMED K, ZHONG J, FAVORS Z, ZAERA F, OZKAN M, OZKAN C S. Hydrous ruthenium oxide nanoparticles anchored to graphene and carbon nanotube hybrid foam for supercapacitors [J]. Scientific Reports, 2014, 4(12): 4452.
- [47] HU C C, WANG C W, CHANG K H, CHEN M G. Anodic composite deposition of RuO₂/reduced graphene oxide/carbon nanotube for advanced supercapacitors [J]. Nanotechnology, 2015, 26(27): 274004–274008.
- [48] CHOU J C, CHEN Y L, YANG M H, CHEN Y Z, LAI C C, CHIU H T, LEE C Y, CHUEH Y L, GAN J Y. RuO₂/MnO₂ core-shell nanorods for supercapacitors [J]. Jmaterchema, 2013, 1(31): 8753–8758.
- [49] RAKHI R B, WEI C, HEDHILI M N, DONGKYU C, ALSHAREEF H N. Enhanced rate performance of mesoporous Co₃O₄ nanosheet supercapacitor electrodes by hydrous RuO₂ nanoparticle decoration [J]. Acs Applied Materials & Interfaces, 2014, 6(6): 4196–4206.
- [50] BRUMBACH M T, ALAM T M, NILSON R H, KOTULA P G, MCKENZIE B B, TISSOT R G, BUNKER B C. Ruthenium oxide-niobium hydroxide composites for pseudocapacitor electrodes [J]. Materials Chemistry and Physics, 2010, 124(1): 359–370.
- [51] DESHMUKH P R. Polyaniline-RuO₂ composite for high performance supercapacitors: chemical synthesis and properties [J]. Rsc Advances, 2015, 5(36): 28687–28695.
- [52] DESHMUKH P R, PATIL S V, BULAKHE R N, SARTALE S D, LOKHANDE C D. Inexpensive synthesis route of porous polyaniline–ruthenium oxide composite for supercapacitor application [J]. Chemical Engineering Journal, 2014, 257(8): 82–89.
- [53] CHO S, KIM M, JANG J. Screen-printable and flexible RuO₂ nanoparticle-decorated PEDOT:PSS/graphene nanocomposite with enhanced electrical and electrochemical performances for high-capacity supercapacitor [J]. Acs Applied Materials & Interfaces, 2015, 7(19): 11–17.
- [54] LEE J W, AHN T, KIM J H, KO J M, KIM J D. Nanosheets based mesoporous NiO microspherical structures via facile and template-free method for high performance supercapacitors [J]. Electrochimica Acta, 2011, 56(13): 4849–4857.
- [55] DING S, ZHU T, CHEN J S, WANG Z, YUAN C, LOU X W. Controlled synthesis of hierarchical NiO nanosheet hollow spheres with enhanced supercapacitive performance [J]. Journal of Materials Chemistry, 2011, 21(18): 6602–6606.
- [56] LI Y, TAN B, WU Y. Ammonia-evaporation-induced synthetic method for metal (Cu, Zn, Cd, Ni) hydroxide/oxide nanostructures [J]. Chemistry of Materials, 2008, 20(7): 567–576.
- [57] XI W, YU L, PENG H, YUAN F. Synthesis of single-crystalline

- hollow octahedral NiO [J]. Crystal Growth & Design, 2007, 7(12): 2415-2418.
- [58] BIJU V, KHADAR M A. AC conductivity of nanostructured nickel oxide [J]. Journal of Materials Science, 2001, 36(24): 5779–5787.
- [59] ZHANG X, SHI W, ZHU J, ZHAO W, MA J, MHAISALKAR S, MARIA T L, YANG Y, ZHANG H, HNG H H. Synthesis of porous NiO nanocrystals with controllable surface area and their application as supercapacitor electrodes [J]. Nano Research, 2010, 3(9): 643–652.
- [60] VIJAYAKUMAR S, NAGAMUTHU S, MURALIDHARAN G. Supercapacitor studies on NiO nanoflakes synthesized through a microwave route [J]. Acs Applied Materials & Interfaces, 2013, 5(6): 2188–2196.
- [61] WANG H, YI H, CHEN X, WANG X. Asymmetric supercapacitors based on nano-architectured nickel oxide/graphene foam and hierarchical porous nitrogen-doped carbon nanotubes with ultrahighrate performance [J]. Journal of Materials Chemistry A, 2014, 2(9): 3223–3230
- [62] LU Q. Supercapacitor electrodes with high-energy and power densities prepared from monolithic NiO/Ni Nanocomposite [J]. Angewandte Chemie International Edition, 2011, 50(30): 6847–6850
- [63] WANG H, CASALONGUE H S, LIANG Y, DAI H. Ni(OH)₂ nanoplates grown on graphene as advanced electrochemical pseudocapacitor materials [J]. Journal of the American Chemical Society, 2010, 132(21): 7472-7.
- [64] KONG X, LIU X, HE Y, ZHANG D, WANG X, LI Y. Hydrothermal synthesis of β -nickel hydroxide microspheres with flakelike nanostructures and their electrochemical properties [J]. Materials Chemistry & Physics, 2007, 106(106): 375-8.
- [65] WANG X F, RUAN D B, YOU Z. Application of spherical Ni(OH)₂/CNTs composite electrode in asymmetric supercapacitor [J]. Transactions of Nonferrous Metals Society of China, 2006, 16(5): 1129–1134.
- [66] MATSUI K, KYOTANI T, TOMITA A. Hydrothermal synthesis of single-crystal Ni(OH)₂ nanorods in a carbon-coated anodic alumina film [J]. Advanced Materials, 2002, 14(17): 1216–1219.
- [67] CHENG Q, TANG J, MA J, ZHANG H, SHINYA N, QIN L C. Graphene and nanostructured MnO₂ composite electrodes for supercapacitors [J]. Carbon, 2011, 49(9): 2917–2925.
- [68] YAN J, FAN Z, WEI S, NING G, TONG W, QIANG Z, ZHANG R, ZHI L, FEI W. Advanced asymmetric supercapacitors based on Ni(OH)₂/graphene and porous graphene electrodes with high energy density [J]. Advanced Functional Materials, 2012, 22(12): 2632–2641.
- [69] SUN X, WANG G, HWANG J Y, LIAN J. Porous nickel oxide nano-sheets for high performance pseudocapacitance materials [J]. Journal of Materials Chemistry, 2011, 21(41): 16581–16588.
- [70] MATHIEU T, THIERRY B, DANIEL B L. Charge storage mechanism of MnO₂ electrode used in aqueous electrochemical capacitor [J]. Chemistry of Materials, 2004, 16(16): 3184–3190.
- [71] LEE H Y, GOODENOUGH J B. Supercapacitor behavior with KCl electrolyte [J]. Journal of Solid State Chemistry, 1999, 144(1): 220–223.
- [72] YANG X H, WANG Y G, XIONG H M, XIA Y Y. Interfacial synthesis of porous MnO₂ and its application in electrochemical capacitor [J]. Electrochimica Acta, 2007, 53(2): 752–757.
- [73] PANG S C, ANDERSON M A. Novel electrode materials for thin-film ultracapacitors: Comparison of electrochemical properties of sol-gel-derived and electrodeposited manganese dioxide [J]. Journal of the Electrochemical Society, 2000, 147(2): 444-50.

950-955

- [74] KANG J, CHEN L, HOU Y, LI C, FUJITA T, LANG X, HIRATA A, CHEN M. Electroplated thick manganese oxide films with ultrahigh capacitance [J]. Advanced Energy Materials, 2013, 3(7): 857–63.
- [75] ZHANG Y, LIU K Y, ZHANG W, SU Geng. Performance of positive and negative electrodes in amorphous manganese oxide supercapacitor [J]. Transactions of Nonferrous Metals Society of China, 2007, 17(S1): 1014–1017.
- [76] CHANG J K, TSAI W T. Material characterization and electrochemical performance of hydrous manganese oxide electrodes for use in electrochemical pseudocapacitors [J]. Historia Mathematica, 1997, 24(3): 301–31.
- [77] LANG X, HIRATA A, FUJITA T, CHEN M. Nanoporous metal/oxide hybrid electrodes for electrochemical supercapacitors [J]. Nature Nanotechnology, 2011, 6(4): 232–236.
- [78] WANG W, GUO S, BOZHILOV K N, YAN D, OZKAN M, OZKAN C S. Intertwined nanocarbon and manganese oxide hybrid foam for high-energy supercapacitors [J]. Small, 2013, 9(21): 3714–3721.
- [79] RUI X, ZHU J, LIU W, TAN H, SIM D, XU C, ZHANG H, MA J, HNG H H, LIM T M. Facile preparation of hydrated vanadium pentoxide nanobelts based bulky paper as flexible binder-free cathodes for high-performance lithium ion batteries [J]. Rsc Advances, 2011, 1(1): 117–122.
- [80] XIONG C, ALIEV A E, GNADE B, BALKUS K J. Fabrication of silver vanadium oxide and V₂O₅ nanowires for electrochromics [J]. Acs Nano, 2008, 2(2): 293–301.
- [81] YU D, CHEN C, XIE S, LIU Y, PARK K, ZHOU X, ZHANG Q, LI J, CAO G. Mesoporous vanadium pentoxide nanofibers with significantly enhanced Li-ion storage properties by electrospinning [J]. Energy & Environmental Science, 2011, 4(3): 858–861.
- [82] LI M, KONG F, WANG H, LI G. Synthesis of vanadium pentoxide (V_2O_5) ultralong nanobelts via an oriented attachment growth mechanism [J]. Crystengcomm, 2011, 13(17): 5317–5320.
- [83] WU C Z, XIE Y, LEI L Y, HU S Q, OUYANG C Z. Synthesis of new-phased VOOH hollow "dandelions" and their application in lithium-ion batteries [J]. Advanced Materials, 2006, 18(13): 1727–1732.
- [84] ŚWIATOWSKA-MROWIECKA J, MAURICE V, ZANNA S, KLEIN L, MARCUS P. XPS study of Li ion intercalation in V_2O_5 thin films prepared by thermal oxidation of vanadium metal [J]. Electrochimica Acta, 2007, 52(18): 5644–5653.
- [85] WEI Y, ZHU J, WANG G. High-specific-capacitance supercapacitor based on vanadium oxide nanoribbon [J]. IEEE Transactions on Applied Superconductivity, 2014, 24(5): 1–4.
- [86] STOLLER M D, PARK S, ZHU Y, AN J, RUOFF R S. Graphene-based ultracapacitors [J]. Nano Letters, 2008, 8(10): 3498–3502.
- [87] WANG Y, SHI Z, HUANG Y, MA Y, WANG C, CHEN M, CHEN Y. Supercapacitor devices based on graphene materials [J]. Journal of Physical Chemistry C, 2009, 113(30): 13103–13107.
- [88] YE G, GONG Y, KEYSHAR K, HUSAIN E A M, BRUNETTO G, YANG S, VAJTAI R, AJAYAN P M. 3D reduced graphene oxide coated V₂O₅ nanoribbon scaffolds for high-capacity supercapacitor electrodes [J]. Particle & Particle Systems Characterization, 2015, 32(8): 817–821.
- [89] CHEN Z, AUGUSTYN V, WEN J, ZHANG Y, SHEN M, DUNN B, LU Y. High-performance supercapacitors based on intertwined CNT/V₂O₅ nanowire nanocomposites [J]. Advanced Materials, 2011, 23(6): 791–795.
- [90] QU Q, ZHU Y, GAO X, WU Y. Core–shell structure of polypyrrole grown on V_2O_5 nanoribbon as high performance anode material for supercapacitors [J]. Advanced Energy Materials, 2012, 2(8):

- [91] KADAM L D, PATIL P S. Thickness-dependent properties of sprayed cobalt oxide thin films [J]. Materials Chemistry & Physics, 2001, 68: 225–232.
- [92] LU Z, YANG Q, ZHU W, CHANG Z, LIU J, SUN X, EVANS D G, DUAN X. Hierarchical Co₃O₄@Ni-Co-O supercapacitor electrodes with ultrahigh specific capacitance per area [J]. Nano Research, 2012, 5(5): 369-378.
- [93] SHINDE V R, MAHADIK S B, GUJAR T P, LOKHANDE C D. Supercapacitive cobalt oxide (Co₃O₄) thin films by spray pyrolysis [J]. Applied Surface Science, 2006, 252(20): 7487–92.
- [94] XIE L, LI K, SUN G, HU Z, LV C, WANG J, ZHANG C. Preparation and electrochemical performance of the layered cobalt oxide (Co₃O₄) as supercapacitor electrode material [J]. Journal of Solid State Electrochemistry, 2013, 17(1): 55–61.
- [95] GAO Y, CHEN S, CAO D, WANG G, YIN J. Electrochemical capacitance of Co₃O₄ nanowire arrays supported on nickel foam [J]. Journal of Power Sources, 2010, 195(6): 1757–1760.
- [96] BARRERA-CALVA E, MART NEZ-FLORES J C, HUERTA L, AVILA A, ORTEGA-L PEZ M. Ellipsometric spectroscopy study of cobalt oxide thin films deposited by sol-gel [J]. Solar Energy Materials & Solar Cells, 2006, 90(15): 2523–2531.
- [97] LIAO C L, WU M T, YEN J H, LEU I C, FUNG K Z. Preparation of RF-sputtered lithium cobalt oxide nanorods by using porous anodic alumina (PAA) template [J]. Journal of Alloys & Compounds, 2006, 414(1-2): 302-309.
- [98] CUI L, LI J, ZHANG X G. Preparation and properties of Co₃O₄ nanorods as supercapacitor material [J]. Journal of Applied Electrochemistry, 2009, 39(10): 1871–1876.
- [99] WEI T Y, CHEN C H, CHANG K H, LU S Y, HU C C. Cobalt oxide aerogels of ideal supercapacitive properties prepared with an epoxide synthetic route [J]. Chemistry of Materials, 2009, 21(14): 3228–3233.
- [100] ZHANG H, YU X, BRAUN P V. Three-dimensional bicontinuous ultrafast-charge and-discharge bulk battery electrodes [J]. Nature Nanotechnology, 2011, 6(5): 277–281.
- [101] LEI Z, LU L, ZHAO X S. The electrocapacitive properties of graphene oxide reduced by urea [J]. Energy & Environmental Science, 2012, 5(4): 6391–6399.
- [102] WANG H, LIANG Y, MIRFAKHRAI T, CHEN Z, CASALONGUE H S, DAI H. Advanced asymmetrical supercapacitors based on graphene hybrid materials [J]. Nano Research, 2011, 4(8): 729–736.
- [103] DONG X C, XU H, WANG X W, HUANG Y X, CHAN-PARK M B, ZHANG H, WANG L H, HUANG W, CHEN P. 3D graphene-cobalt oxide electrode for high-performance supercapacitor and enzymeless glucose detection [J]. Acs Nano, 2012, 6(4): 3206–3213.
- [104] WANG X, YAN C, SUMBOJA A, LEE P S. High performance porous nickel cobalt oxide nanowires for asymmetric supercapacitor [J]. Nano Energy, 2013, 3(1): 119–126.
- [105] GUPTA V, GUPTA S, MIURA N. Al-substituted α-cobalt hydroxide synthesized by potentiostatic deposition method as an electrode material for redox-supercapacitors [J]. Journal of Power Sources, 2008, 177(177): 685–689.
- [106] LI R, HU Z, SHAO X, CHENG P, LI S, YU W, LIN W, YUAN D. Large scale synthesis of NiCo layered double hydroxides for superior asymmetric electrochemical capacitor [J]. Scientific Reports, 2016, 6(18):73-77
- [107] ZHOU W J, XU M W, ZHAO D D, XU C L, LI H L. Electrodeposition and characterization of ordered mesoporous cobalt hydroxide films on different substrates for supercapacitors [J]. Microporous & Mesoporous Materials, 2009, 117(1–2): 55–60.

- [108] HORKANS J, SHAFER M W. An investigation of the electrochemistry of a series of metal dioxides with rutile-type structure: MoO₂, WO₂, ReO₂, RuO₂, OsO₂, and IrO₂ [J]. Journal of the Electrochemical Society, 1977, 124(8): 1202–1207.
- [109] OLIVEIRA-SOUSA A D, SILVA M A S D, MACHADO S A S, AVACA L A, LIMA-NETO P D. Influence of the preparation method on the morphological and electrochemical properties of Ti/IrO₂coated electrodes [J]. Electrochimica Acta, 2000, 45(27): 4467–4473.
- [110] LIU D Q, YU S H, SON S W, JOO S K. Electrochemical performance of iridium oxide thin film for supercapacitor prepared by radio frequency magnetron sputtering method [J]. Ecs Transactions, 2008, 16(1).
- [111] GRUPIONI A A F, ARASHIRO E, LASSALI T A F. Voltammetric characterization of an iridium oxide-based system: The pseudocapacitive nature of the $Ir_{0.3}Mn_{0.7}O_2$ electrode [J]. Electrochimica Acta, 2002, 48(4): 407–418.
- [112] SHAO Y Q, YI Z Y, HE C, ZHU J Q, TANG D. Effects of annealing temperature on the structure and capacitive performance of nanoscale Ti/IrO₂–ZrO₂ electrodes [J]. Journal of the American Ceramic Society, 2015, 98(5): 1485–1492.
- [113] CHEN Y M, HUANG Y S, LEE K Y, TSAI D S, TIONG K K. Characterization of IrO₂/CNT nanocomposites [J]. Journal of Materials Science Materials in Electronics, 2011, 22(7): 890–894.
- [114] SHIH Y T, LEE K Y, HUANG Y S. Characterization of iridium dioxide–carbon nanotube nanocomposites grown onto graphene for supercapacitor [J]. Journal of Alloys & Compounds, 2015, 619: 131–137.
- [115] VOLPE L, BOUDART M. Compounds of molybdenum and tungsten with high specific surface area: II. Carbides [J]. Journal of Solid State Chemistry, 1985, 59(3): 348–356.
- [116] GIORDANO C, ANTONIETTI M. Synthesis of crystalline metal nitride and metal carbide nanostructures by sol-gel chemistry [J]. Nano Today, 2011, 6(6): 366–380.
- [117] YAO W, MAKOWSKI P, GIORDANO C, GOETTMANN F. Synthesis of early-transition-metal carbide and nitride nanoparticles through the urea route and their use as alkylation catalysts [J]. Chemistry - A European Journal, 2009, 15(44): 11999–112004.
- [118] BOUHTIYYA S, LUCIOPORTO R, DUCROS J B, BOULET P, CAPON F, BROUSSE T, PIERSON J F. Transition metal nitrides thin films for supercapacitor applications [J]. 2012, 48(5): 43–49.
- [119] LI X, SUN Y, ZHANG Y, CAO M. Facile preparation of mesoporous titanium nitride microspheres as novel adsorbent for trace Cd²⁺ removal from aqueous solution [J]. Journal of Physics & Chemistry of Solids, 2015, 81: 22–26.
- [120] DONG S, CHEN X, LIN G, ZHOU X, XU H, WANG H, LIU Z, HAN P, YAO J, WANG L. Facile preparation of mesoporous titanium nitride microspheres for electrochemical energy storage [J]. Acs Applied Materials & Interfaces, 2011, 3(1): 93–98.
- [121] XIE Y, WANG Y, DU H. Electrochemical capacitance performance of titanium nitride nanoarray [J]. Materials Science & Engineering B, 2013. 178(20): 1443–1451.
- [122] PENG X, HUO K, FU J, ZHANG X, GAO B, CHU P K. Coaxial PANI/TiN/PANI nanotube arrays for high-performance supercapacitor electrodes [J]. Chemical Communications, 2013, 49(86): 10172–10174.
- [123] PENG X, HUO K, FU J, GAO B, WANG L, HU L, ZHANG X, CHU P K. Porous dual-layered MoO_x nanotube arrays with highly conductive TiN cores for supercapacitors [J]. Chem Electro Chem, 2015, 2(4): 512–517.
- [124] XIE Y, FANG X. Electrochemical flexible supercapacitor based on manganese dioxide-titanium nitride nanotube hybrid [J].

- Electrochimica Acta, 2014, 120(7): 273-283.
- [125] SHANG C, DONG S, WANG S, XIAO D, HAN P, WANG X, GU L, CUI G. Coaxial Ni_xCo_{2x}(OH)_{6x}/TiN nanotube arrays as supercapacitor electrodes [J]. Acs Nano, 2013, 7(6): 5430–5436.
- [126] LU X, LIU T, ZHAI T, WANG G, YU M, XIE S, LING Y, LIANG C, TONG Y, LI Y. Improving the cycling stability of metal–nitride supercapacitor electrodes with a thin carbon shell [J]. Advanced Energy Materials, 2014, 4(4): 168–175.
- [127] CHOI D, BLOMGREN G E, KUMTA P N. Cover picture: Fast and reversible surface redox reaction in nanocrystalline vanadium nitride supercapacitors [J]. Advanced Materials, 2006, 18(9): 1178–1182.
- [128] SUN Q, FU Z W. Vanadium nitride as a novel thin film anode material for rechargeable lithium batteries [J]. Electrochimica Acta, 2008, 54(2): 403–409.
- [129] ZHOU X, CHEN H, SHU D, HE C, NAN J. Study on the electrochemical behavior of vanadium nitride as a promising supercapacitor material [J]. Journal of Physics & Chemistry of Solids, 2009, 70(2): 495–500.
- [130] GLUSHENKOV A M, HULICOVAJURCAKOVA D, LLEWELLYN D, LU G Q, CHEN Y. Structure and capacitive properties of porous nanocrystalline VN prepared by temperature-programmed ammonia reduction of V₂O₅† [J]. Chemistry of Materials, 2010, 22(3): 914–921
- [131] SU Y, ZHITOMIRSKY I. Hybrid MnO₂/carbon nanotube-VN/carbon nanotube supercapacitors [J]. Journal of Power Sources, 2014, 267(3): 235–242
- [132] DONG S, CHEN X, GU L, ZHOU X, WANG H, LIU Z, HAN P, YAO J, WANG L, CUI G. TiN/VN composites with core/shell structure for supercapacitors [J]. Materials Research Bulletin, 2011, 46(6): 835–839.
- [133] ZHANG L, HOLT C M B, LUBER E J, OLSEN B C, WANG H, DANAIE M, CUI X, TAN X H, LUI V W, KALISVAART W P. High rate electrochemical capacitors from three-dimensional arrays of vanadium nitride functionalized carbon nanotubes [J]. Jphyschemc, 2011, 115(49): 24381–24393.
- [134] FINELLO D. New developments in ultracapacitor technology [R].Wright Lab, Eglin AFB, FL, USA, 1995.
- [135] LIU T C. Behavior of molybdenum nitrides as materials for electrochemical capacitors [J]. Journal of the Electrochemical Society, 1998, 145(6): 1882–1888.
- [136] LI X L, XING Y, WANG H. Synthesis and characterization of uniform nanoparticles of γ-Mo₂N for supercapacitors [J]. Transactions of Nonferrous Metals Society of China, 2009, 19(3): 620–625.
- [137] GANIN A Y, KIENLE L, VAJENINE G V. Synthesis and characterisation of hexagonal molybdenum nitrides [J]. Journal of Solid State Chemistry, 2006, 179(8): 2339–2348.
- [138] SHAH S I U, HECTOR A L, OWEN J R. Redox supercapacitor performance of nanocrystalline molybdenum nitrides obtained by ammonolysis of chloride- and amide-derived precursors [J]. Journal of Power Sources, 2014, 266(1): 456–463.
- [139] WEN M A, HAN P X, SHAN K Q, ZHANG K J, FENG B C, LEI C G. Study on the MoN/nitrogen-doped graphene sheets composite for lithium ion capacitor electrode materials [J]. Journal of Inorganic Materials, 2013, 28(7): 733–738.
- [140] WEN M, HU C Q, MENG Q N, ZHAO Z D, AN T, SU Y D, YU W X, ZHENG W T. Effects of nitrogen flow rate on the preferred orientation and phase transition for niobium nitride films grown by direct current reactive magnetron sputtering [J]. Journal of Physics D: Applied Physics, 2008, 42(3): 305–310.
- $[141] \ \ CUI \ Hou-lei, ZHU \ Gui-lian, LIU \ Xiang-ye, LIU \ Feng-xin, XIE \ Yian.$

- Niobium nitride Nb_4N_5 as a new high-performance electrode material for supercapacitors [J]. Advanced Science, 2015, 2(12): 2–10
- [142] DAS B, BEHM M, LINDBERGH G, REDDY M V, CHOWDARI B V R. High performance metal nitrides, MN (M=Cr, Co) nanoparticles for non-aqueous hybrid supercapacitors [J]. Advanced Powder
- Technology, 2015, 26(3): 783-788.
- [143] BOUHTIYYA S, PORTO R L, LA K B, BOULET P, CAPON F, PEREIRA-RAMOS J P, BROUSSE T, PIERSON J F. Application of sputtered ruthenium nitride thin films as electrode material for energy-storage devices [J]. Scripta Materialia, 2013, 68(9): 659–662.

过渡金属氧/氮化物赝电容器电极材料的研究进展

易琛琦, 邹俭鹏, 杨洪志, 冷 娴

中南大学 粉末冶金国家重点实验室,长沙 410083

摘 要:法拉第赝电容器兼具二次电池高能量密度和超级电容器高功率密度的优点,而电极材料是决定法拉第赝电容器性能的关键。过渡金属氧化物/氮化物作为两种主要的赝电容器电极材料,能在提高能量密度的同时保持高功率密度。本文综述钌氧化物、镍氧化物、锰氧化物、钒氧化物、钴氧化物、铱氧化物等过渡金属氧化物和钛氮化物、钒氮化物、钼氮化物、铌氮化物等过渡金属氮化物的纳米结构设计和高比表面积复合材料制备的最新进展,为法拉第赝电容器电极材料的深入研究提供重要的借鉴意义。

关键词: 赝电容器; 过渡金属氧化物; 过渡金属氮化物; 功率密度; 能量密度

(Edited by Xiang-qun LI)